



TAMPEREEN TEKNILLINEN YLIOPISTO
TAMPERE UNIVERSITY OF TECHNOLOGY

JANNE RUUSKANEN

**PREDICTING HEAT PROPAGATION IN ROEBEL CABLE BASED
ACCELERATOR MAGNET PROTOTYPE**

Master of Science thesis

Examiners: Project manager
Antti Stenvall and Post-doctoral
researcher Valtteri Lahtinen

The examiners and topic of the the-
sis were approved on 5 October
2016

ABSTRACT

JANNE RUUSKANEN: Predicting Heat Propagation in Roebel Cable Based Accelerator Magnet Prototype

Tampere University of Technology

Master of Science thesis, 54 pages

June 2017

Master's Degree Programme in Electrical Engineering

Major: Electromagnetics

Examiners: Project manager Antti Stenvall and Post-doctoral researcher Valtteri Lahtinen

Keywords: Accelerator magnets, Finite element methods, HTS cables, Quench

Superconductors are a tempting alternative to be used in high-current applications due to their property of lossless current carrying ability. The high material costs and laborious fabrication processes, however, prevent the more common use in different suitable application areas. Presently, several research and development projects use superconductors. One of the applications is the Large Hadron Collider (LHC) particle accelerator in the European Organization for Nuclear Research (CERN). In LHC, superconductor based electromagnets for particle beam steering and focusing are utilized.

Superconductors can carry direct current without heat losses only if the current, magnetic field and temperature are below certain boundary, the critical surface. Otherwise the superconductor becomes resistive and heat is generated. This can lead to uncontrollable temperature increasing, quench, in the device and actions are needed in order to prevent damages. One must be prepared for quench by designing an adequate protection system for the device. The design can be aided by simulating heat transfer in the device during quench. The simulations can be time consuming in case of large devices consisting of anisotropic materials, like the magnet's in LHC. However, adequate modelling decisions can significantly reduce the simulation time, while leading to results with sufficient accuracy. This involves identifying the essential interplaying physical phenomena and choosing an appropriate representation for the modelling domain.

In this thesis, quench modelling of superconducting magnets is discussed. Moreover, a simulation tool was developed for quench simulations suitable for large superconducting devices. The tool utilizes a novel numerical approach to solve three-dimensional (3-D) heat diffusion in one-dimensional (1-D) modelling domain. To study the capability of the simulation tool, quench analysis was performed for an accelerator magnet prototype. The tool was able to solve the heat transfer during a quench in the magnet in couple of minutes while the same problem utilizing conventional 3-D modelling domain would take several hours even. Furthermore, to study the prospects of utilizing this new approach in quench protection design, comparison with measurement data is needed.

PREFACE

This is a reprint of master's thesis submitted in 2017 at Tampere University of Technology for the partial fulfilment for the degree of Master's of Technology.

CONTENTS

1.	INTRODUCTION	1
2.	INTRODUCTION TO TECHNICAL SUPERCONDUCTORS	2
2.1	Early days of superconductivity.....	2
2.1.1	Discovery of superconductivity	2
2.1.2	Towards superconducting materials for large scale applications..	3
2.2	Conductors	4
2.2.1	LTS wires.....	4
2.2.2	HTS wires	6
2.2.3	Losses in technical superconductors.....	8
2.3	Cables.....	9
2.3.1	Rutherford cable	9
2.3.2	Cable-in-conduit conductor	10
2.3.3	Roebel cable.....	11
2.3.4	Other cable developments.....	12
2.4	Applications	13
2.5	Remarks	14
3.	SUPERCONDUCTOR STABILITY	15
3.1	Disturbance spectrum.....	15
3.2	Quench	16
3.3	Stability margins	17
3.4	Quench protection.....	18
3.4.1	Energy extraction with dump resistor	19
3.4.2	Protection heaters.....	20
3.4.3	CLIQ.....	20
3.4.4	E ³ SPreSSO	21
3.4.5	ICED	21
4.	QUENCH MODELLING	23
4.1	Quench as a multiphysics problem	23
4.1.1	Modelling decisions.....	25
4.2	Approaches to model quench propagation.....	26
4.2.1	Solving heat diffusion equation	27
4.2.2	Tabular approach.....	27
4.2.3	Heat generation.....	27
4.3	Material properties	30
4.3.1	Effective material properties.....	30
4.3.2	Representing the critical surface.....	31
4.4	Numerical methods	32
4.4.1	Finite element method	33
4.4.2	Finite difference method.....	33

4.5	Remarks	34
5.	THE QUENCH SIMULATION TOOL	35
5.1	Included physics and modelling decisions.....	35
5.2	Computational approach and numerical method	36
5.2.1	FEM-FDM hybrid method.....	36
5.2.2	Inputs	37
5.3	Remarks	38
6.	PREDICTING HEAT PROPAGATION IN FEATHER-M0.....	39
6.1	Description of FM0 and quench modelling case	39
6.1.1	Modelling domain.....	39
6.1.2	Material properties.....	40
6.1.3	Heat generation.....	40
6.1.4	Quench protection.....	40
6.2	Simulation results.....	41
6.2.1	An analysis of the nominal quench.....	41
6.2.2	Critical current of the coil.....	42
6.2.3	Varying detection voltage and switch delay	46
7.	CONCLUSIONS	48
	REFERENCES	49

LIST OF SYMBOLS AND ABBREVIATIONS

A_{stab}	Cross-sectional area of stabilizer
\mathbf{B}	Vector field representation of magnetic flux density
B	magnitude of \mathbf{B}
B_c	Critical magnetic flux density
B_{c1}	Lower critical magnetic flux density
B_{c2}	Upper critical magnetic flux density
C	Volumetric specific heat
C_{eff}	Effective C
D	System matrix in FDM
\mathbf{E}	Vector field representation of electric field
E	Magnitude of \mathbf{E}
E_c	Electric field criterion
e	Element in FEM discretization
f	Material proportion
I	Current
I_c	Critical current
I_{op}	Operation current
I_{sc}	Current in superconducting region
I_{stab}	Current in the stabilizer region
\mathbf{J}	Vector field representation of current density
J	Magnitude of \mathbf{J}
J_c	Critical current density
J_{c0}	J_c at T_0
J_{ec}	Engineering critical current density
K	Stiffness matrix
L	Inductance
L_{nz}	Length of normal zone
M	Mass matrix
n	The n -value of superconductor in the power-law
N	Integer
P_{PH}	Protection heater surface power
\mathbf{q}	Heat flux
Q	Heat generation
\mathbf{Q}	Load vector
\mathbf{r}	Vector of coordinates
R_{coil}	Normal zone resistance over superconducting winding
R_d	Resistance of dump resistor
Δr	Thickness of insulation layer between cable turns
T	Temperature
\mathbf{T}	A vector of temperatures

$\dot{\mathbf{T}}$	Element-wise time derivative of \mathbf{T}
T_c	Critical temperature
T_{cs}	Current sharing temperature
T_{op}	Operation temperature
T_0	Initial temperature
t	Time
t_{del}	Quench protection system activation delay
V	Voltage
v_{nzp}	Normal zone propagation velocity
v_c	Voltage over normal zone
V_{det}	Quench detection voltage
Δt	Time step
λ	Thermal conductivity
λ_{eff}	Effective λ
ρ	Resistivity
ρ_{eff}	Effective ρ
τ	Time constant
ρ_{stab}	Resistivity of the matrix metal
Δ	Difference/Distance
θ	Angle in degrees
Ω	Modelling domain
ψ	Basis functions in FEM
AC	Alternating current
Al	Aluminum
BSCCO	Bismuth based high temperature superconductors
CERN	the European Organization for Nuclear Research
CICC	cable-in-conduit conductor
CLIQ	The Coupling-Loss Induced Quench, a protection system
CORC	Conductor on round core
CuTi	Copper titanium, material compound
DC	Constant current (direct current)
DoF	Degrees of freedom
E ³ SPreSSO	Energy Extraction Symbiotic Protection System for Series Operation, a quench protection method
EuCARD-2	Enhanced European Coordination for Accelerator Research & Development
FCL	Fault current limiter
FDM	Finite difference method
FEM	Finite element method

FDM	Finite difference method
FM0	Feather-M0, HTS accelerator magnet prototype
GdBCO	Gadolinium barium copper oxide, an HTS material
G10	Fibre glass compound
Hg	Mercury
HTS	High temperature superconductor
ICED	Inductively coupled energy dissipator, a quench protection method
IVP	Initial value problem
LHC	Large Hadron Collider, a particle accelerator
LTS	Low temperature superconductor
MagLab	The National High Magnetic Field Laboratory
MgB ₂	Magnesium diboride, an HTS material
MPZ	Minimum propagation zone
MRI	Magnetic resonance imaging
MQE	Minimum quench energy
NbTi	Niobium titanium, an LTS material
Nb ₃ Sn	Niobium tin, an LTS material
PIT	powder in tube method, superconductor fabrication method
R&D	Research and Development
REBCO	rare-earth barium copper oxide, rare-earth compound based HTS material
SMES	Superconducting magnetic energy storage
Sn	Tin
x-D	x-dimensional, where x denotes the dimension 1, 2 or 3
YBCO	Yttrium barium copper oxide, an HTS material

1. INTRODUCTION

Superconductors have ability to carry electric current without heat loss generation. This property makes them favorable for applications. One very important application area, where superconductors are used, is in producing magnetic fields required in accelerator complexes, such as Large Hadron Collider (LHC) in the European Organization for Nuclear Research [10] (CERN). Due to a disturbance, like particle shower or heat leak, the superconducting accelerator magnets, used to steer and squeeze the particle beams, can lose their superconducting state and become resistive. Due to high operation currents massive heat generation can occur. Therefore the highly expensive magnets are likely to be destroyed.

To ensure safe operation and to design magnet protection systems for situations where the superconducting state is lost, modelling is needed. Superconducting devices, like magnets are large in size and consist of anisotropic materials. Therefore modelling heat diffusion in such devices can be time consuming especially if three dimensional modelling domain is utilized. To be able to simulate consequences of uncontrollable heat generation, quench, in highly detailed devices in a reasonable time frame, simplifications are needed.

In this thesis, a simulation tool to predict heat propagation during a quench in superconducting devices, based on a new approach suitable for large devices, is developed and presented. The basic idea of the approach is to model heat propagation during a quench in one-dimensional modelling domain representing the centerline of cable, but still take into account the heat diffusion between the cables. Utilizing the simulation tool, thermal analysis are performed for an accelerator magnet.

In chapter 2, a general overview of practical superconductors, cable types and their applications is presented. Chapter 3 leads the reader deeper in to the topic of this thesis via discussion on superconductor stability. The margins to loss of stability in operation are the major concerns in designing a superconductor based device. In chapter 4, different areas of physics related to modelling of heat transfer in superconducting devices from point of view of two main approaches are discussed. In chapter 5, simulation tool based on a new approach for solving heat transfer is presented. In chapter 6, the simulation tool is utilized to perform thermal analysis for an accelerator magnet prototype. Moreover, results with appropriate discussion are presented. Finally in chapter 7, the conclusions are drawn.

2. INTRODUCTION TO TECHNICAL SUPERCONDUCTORS

In this chapter superconductivity from its discovery to the present state-of-the-art of applications is discussed. First, superconductivity phenomenon is described. Then, we present how superconductors can be categorized into two types. It appears that those being of only the other type are useful for making technical superconducting wires to be utilized in applications. We tell what are the most common materials in these wires and what kind of superconducting cables can be made from these wires. Finally, we review the most well-known application areas where superconductors are these days utilized.

2.1 Early days of superconductivity

When the superconducting state of matter was widely reproduced, the potential that superconducting applications could have was soon understood. In the basic science the systematic study of superconducting materials and compounds including their characterization and theoretical work aiming to the understanding of this phenomenon bursted. On the other hand, it turned out to be very difficult to make, e.g., magnet applications from the raw superconducting materials, and it took until 1955 to achieve a superconducting magnet producing 0.7 T at 4.2 K [69]. From then on, it became better and better understood which materials are useful for making superconducting wires and how to make these for different applications. The 1950s and 1960s can be considered as the beginning of engineering superconductor science. Up to know this has evolved in fine detailed conductors, construction methods for applications as well as their design and modelling methodologies with relevant theoretical understanding.

This section concentrates on the early days that then led to the understanding of what kind of materials are useful for engineers and how we describe these materials.

2.1.1 Discovery of superconductivity

Superconductivity was first discovered accidentally by Kamerlingh Onnes in 1911, when he was investigating conductivity of metals in low temperatures. During his experiments for mercury he suddenly remarked that at a certain low temperature¹ the electrical resistance had unmeasurably small values. He observed a characteristic property of su-

¹Actually, he did the first observation when he was studying the properties of metals at 4.2 K, the boiling point helium.

perconducting materials: the loss of resistance in his sample at temperatures below a material-specific critical temperature T_c .

Later in 1933 Walther Meissner and Robert Ochsenfeld discovered another property characterizing superconductivity [35]. This now known phenomenon Meissner effect means that superconductor repels all magnetic field from its interior regardless of if the field was there before the cooling or if it was applied after the cooling. Even though the Meissner effect holds only at very low applied fields², a material is typically classified to be a superconductor if such environment can be made where the material exhibits the Meissner effect and carries electric current losslessly. [36, 50]

Soon it was found that just like at temperatures above T_c , also applied magnetic field on superconducting sample resulted in loss of superconducting state. Further investigations showed that after a certain magnitude of magnetic field, the so-called critical field (B_c), the sample transitioned to resistive. Furthermore it was observed that in the Meissner phase, i.e. below B_c , screening currents appear in a very thin surface layer of the sample, creating a magnetic field cancelling the external one. As a result field inside the superconductor is zero. Conclusively, among perfect conductivity superconductor can be characterized by perfect diamagnetism. [50]

2.1.2 Towards superconducting materials for large scale applications

However, the perfect diamagnetism was discovered to occur mostly in pure elements like Al, Hg, Sn, etc. When superconducting materials were developed and tested, for some materials the Meissner effect did not occur anymore after certain amplitude of magnetic field even though lossless current carrying properties still existed. These certain compounds seemed to be in some kind of intermediate state in terms of flux penetration. However, when applied magnetic field was further increased, the critical field clearly occurred and superconducting state was lost. This type of superconductors thus had the so-called lower critical field (B_{c1}) and upper critical field (B_{c2}). Therefore a classification of superconductivity into two types of superconductors was done: Type I, the ones that exhibit the Meissner effect, and type II exhibiting the Meissner effect only below B_{c1} and the mixed state between B_{c1} and B_{c2} .

In the mixed state magnetic field penetrates into superconductor in the form of flux vortices, flux tubes. In presence of current, Lorentz force is exerted on those vortices resulting in the generation of frictional heat. In order to prevent the motion of vortices, impurities are added artificially to superconductor. The impurities work as so-called pinning centers to which the flux tubes attach, due to lower energy level they obtain, decreasing

²This is typically not the case in the so-called large scale applications where superconductors are typically utilized to either create large magnetic fields or transfer large currents. In these applications only the ability to carry losslessly current matters.

significantly the flux line movement and therefore, superconductors with strong pinning, i.e. hard superconductors [5], can carry high currents in high external magnetic fields - this is favorable for applications. Moreover, the maximal current that the superconductor can carry at certain magnetic field and temperature is called the critical current density (J_c). [27, 50]

In 1957, the microscopic theory of superconductivity, known as the BCS theory [2], proposed by Bardeen, Cooper and Schrieffer, finally described the phenomenon behind infinite conductivity and Meissner effect. The theory states that the resistance free-current is carried by the so-called Cooper pairs that consists of two electrons having opposite momenta and spins [36, 50]. Later on the BCS theory turned out to have its limits, when in 1986 Bednorz and Müller observed a new kind of superconductor having T_c above the limit of 30 K predicted by the theory. This is when the classification to low- and high temperature superconductors (LTS and HTS, respectively) was born. While the classical low- T_c superconductors obey the BCS theory, the high- T_c ones behave in highly anisotropic manner. In the absence of microscopic theory for HTS, only reasonable way to predict the behavior of high- T_c superconductors is to use the phenomenological conventional theories and extend them for anisotropic material. [50]

The better understanding of superconducting properties of different materials made it possible to harness superconductivity into practical conductors to be used in applications.

2.2 Conductors

Conductors are manufactured from type II hard superconductors. Both, LTS and HTS, have their own pros and cons, one possibly more suitable for certain purpose than another. Whether it is LTS or HTS, the material has to be harnessed into practical form. Manufacturing techniques have to be considered according to the superconducting material, in order to make conductors suitable for different purposes. In Figure 2.1, different type of conductors available are presented based on engineering critical current density (J_{ce}) as a function of applied magnetic field at 4.2 K. J_{ce} , the critical current of the wire divided by its cross-sectional area, is a reasonable key ratio to compare performances of different conductors since its independent on the ratio of matrix metal and superconducting material.

Next, based on Figure 2.1 the different conductor types and their manufacturing techniques are drawn using LTS-HTS division.

2.2.1 LTS wires

As can be seen from Figure 2.1, the LTS based conductor NbTi is practical only in low field use having J_{ce} of 100 A/mm² at 10 T. NbTi based conductors, on the other hand, are cheap to manufacture and can be provided in long lengths. Moreover, magnet winding is

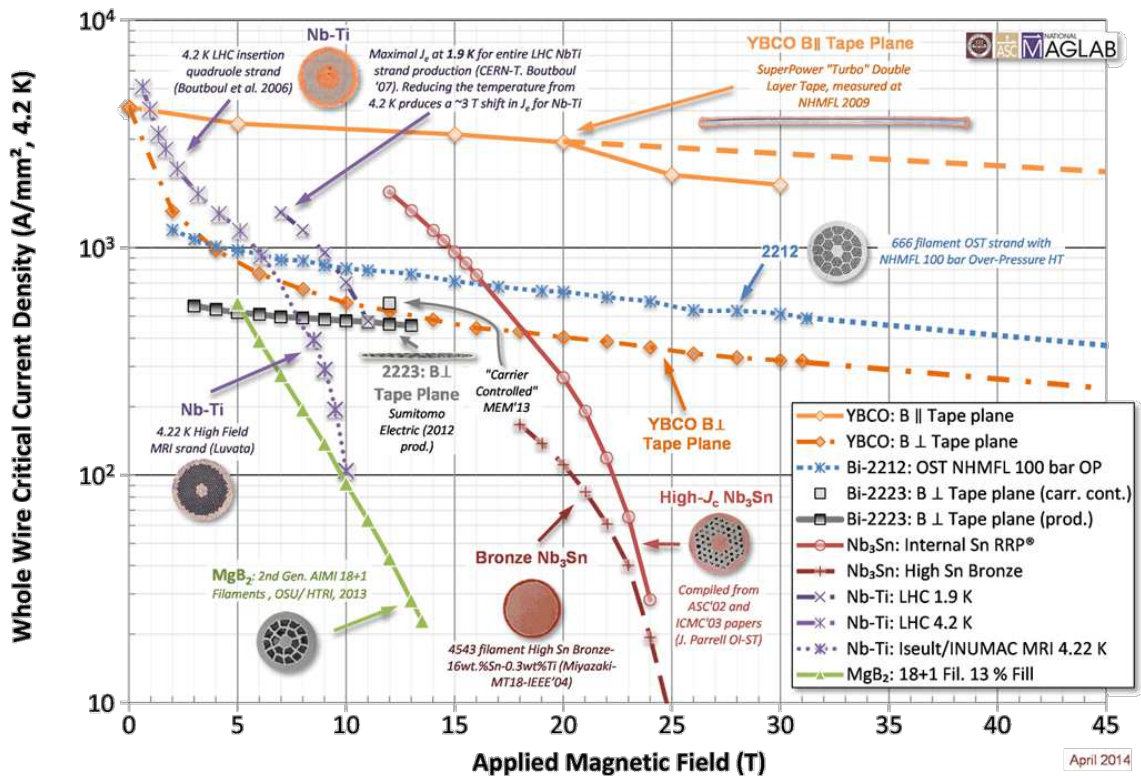


Figure 2.1. Engineering current density as a function of applied magnetic field for present conductor types. Figure by MagLab [32]

easy because they are ductile enough for winding without degradation in superconducting properties.

The manufacturing of NbTi conductors is mainly a cold-working process including various drawing phases where modest heat treatment is applied at the end. The process starts by first producing individual about half meter long round bars which are wrapped into niobium foil. Each of the bars are then slid into a copper tube and processed by heating, compacting, drawing and finally twisted into thin bar of hexagonal cross-section. These bars are cut into about half meter length and stacked inside a copper tube having a copper rod as a center core. After similar processes as in the first phase the bundle is processed to a conductor containing even up to 100,000 NbTi filaments of about 1 μm diameter. Ni foil works as a diffusion barrier between the NbTi and copper in order to prevent CuTi compounds during the process including e.g. heat treatments in high temperatures. [65] In Figure 2.2 cross-section of a NbTi conductor is presented.

From the LTS side the other used compound is Nb₃Sn. As can be seen from Figure 2.1, conductors made of it can reach up to high J_{ce} , of the order of 1000 A/mm² at 10 T, limited to fields around 20 T, however. While Nb₃Sn conductors are better suitable for high field applications, they are very brittle after final heat treatment. Therefore, Nb₃Sn based magnets for example have to be first wound and only after that the heat treatment are done. This makes the magnet fabrication difficult and demanding, naturally

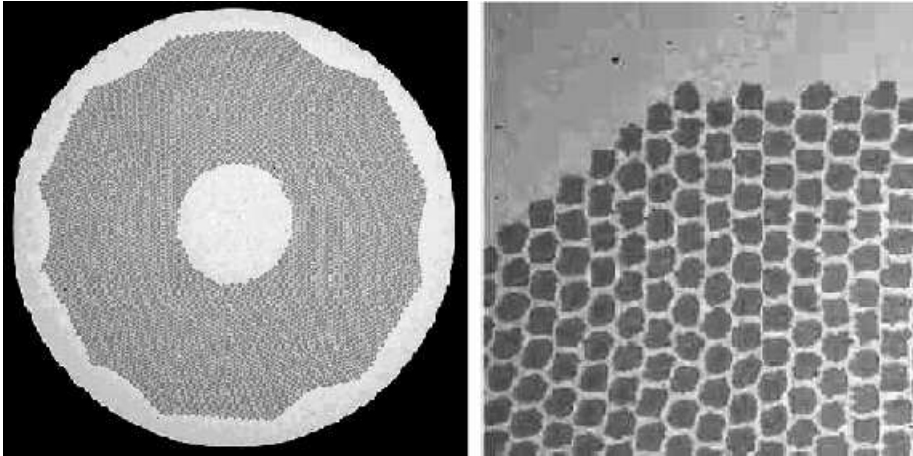


Figure 2.2. Photo of cross-section of a NbTi conductor. Figure from [65].

increasing its costs. [21]

Nb₃Sn wires can be produced in several ways. The most used ones are powder-in-tube method, bronze method and internal-tin method. In bronze method pure niobium filaments, surrounded by diffusion barrier and pure Cu stabilizer, are embedded in CuSn matrix and processed via several heatings and drawings to their final length. Then, during the final heat treatment the tin diffuses to filaments resulting in Nb₃Sn compound. With this method fine filament size (2.5 μm) can be achieved, although, with relatively low J_{ce} compared to, e.g., internal-tin method (IT) [15, 36].

In the IT method the baseline is to have a Sn rod in the center surrounded by Nb rods in pure Cu matrix. This composite covered with diffusion barrier and drawn to a so-called sub-element. The final wire is done by taking a Cu stabilizer tube covered from inside with a diffusion barrier and filled with bundle of sub-elements. This composition is then drawn to final wire and heat processed. In the final heating, the center Sn rod diffuses with the Cu matrix and the the surface of Nb filaments resulting in bronze matrix and superconducting Nb filaments with Nb₃Sn surface layer. [70] The problem in these two methods is, however, that one can achieve either relatively high J_c or fine filaments. Fortunately a new method for having the both, high J_c and fine filaments, was developed for Nb based superconductors, i.e. the powder in tube (PIT) method, where a copper matrix containing Nb tubes filled with Nb₂Sn powder is heat treated. During the heating Nb₃Sn reaction layer is formed but still the high conductivity of the matrix is preserved [36, 59, 66].

2.2.2 HTS wires

Recall that the T_c based division of superconductors classifies them to be high-temperature ones if T_c is above 30 K. As shown in Figure 2.1, on the HTS side are MgB₂ ($T_c = 39$ K), BSCCO ($T_c = 110$ K), and YBCO ($T_c = 93$ K) based conductors. HTS conductors withstand much higher fields than the LTS ones due to their strong pinning. On the

other hand, they are ceramic compounds and therefore brittle. Thus manufacturing these conductors in long lengths is difficult to achieve. However, their performance is favorable in high magnetic field and high current applications.

MgB₂ is an interesting and potential successor for LTS wires towards the higher performance conductors. It is suitable for conduction-cooled applications with low fields at 20-25 K - magnetic resonance imaging use for example. Since sufficient operation temperature for MgB₂ based applications is higher than 4.2 K, expensive liquid helium is not necessary for the cooling, thus liquid hydrogen or cryocoolers can be utilized reducing the cooling expenses. Other benefits are cheap raw materials and easy fabrication. [63]

Bismuth strontium calcium copper oxide (BSCCO) superconducting material was discovered in 1988 [31]. Fabrication of round BSCCO wires can be done with PIT method using silver as matrix metal [37, 48]. Even though the manufacturing technique resembles the LTS one, long lengths are difficult to manufacture due to voids in the structure that decreases I_c – unless high pressure heat treatments are done. In addition, fabricating long lengths of good quality conductors is difficult due to demanding and precise heat treatment that are required. Often, BSCCOs are then processed into tapes by rolling the wire. BSCCO based conductors can typically carry engineering current density of 500 A/mm² at 10 T which is less than YBCO based conductors can carry. However, advantage of BSCCO based ones is the easy and cheaper fabrication of conductors in long unit lengths compared to YBCO tapes. [29]

The REBCOs, rare-earth barium copper oxide, based conductors present the very state-of-the-art of high performance superconducting materials [41]. The commonly used RE-materials are yttrium (Y) and Gadolinium (Gd) resulting in YBCO and GdBCO compounds, respectively [42]. They are known also as the second generation HTS wires that are the most promising conductors for high field applications [51]. REBCO based wires are typically very thin tapes having aspect ratio of the order of 6 or even higher. Structure of a single REBCO tape is shown in Figure 2.3. These wires consist of several different layers: Copper stabilizer and silver layer on both sides, substrate that is typically hastelloy, buffer layer and the actual superconducting layer - REBCO. Due to their structure, they are also called coated conductors. Tapes are manufactured using thin film deposition techniques that are used also in semiconductor industry. In global markets there exist several producers like SuperPower, Superox, American Superconductor Corporation and Fujikura [1, 13, 57, 58], to name some. YBCO based conductors can reach up to J_{ce} of over 1000 A/mm² in magnetic fields up to even 30 T, which makes them suitable for high field applications. However, they are difficult and expensive to fabricate due the complexity of the process. Even though YBCO coated conductors are also highly anisotropic, they are considered to be the most promising superconductors for high-current applications. [51]

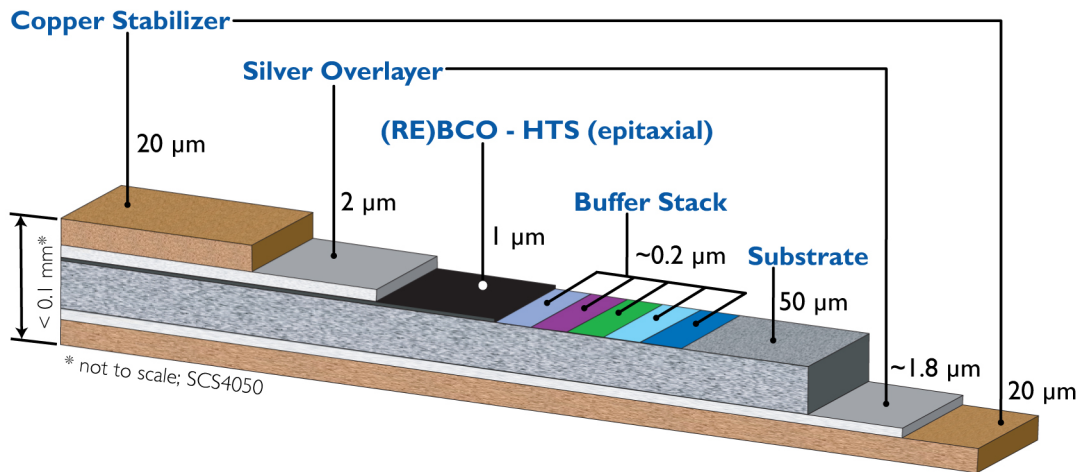


Figure 2.3. Structure of a REBCO tape. Figure from [58].

2.2.3 Losses in technical superconductors

Technical superconductors, the ones used in applications, are hard superconductors, they however have one remarkable undesired property, namely alternating current (AC) losses. These losses occur only in AC operation, i.e., if applied current or the external magnetic field changes in time. AC losses in superconducting wires can be categorized into three: eddy current losses, coupling losses and hysteresis losses. Eddy current and coupling losses are a matter of the resistive stabilizer metal of the superconductor wire. Eddy current losses are generated when conducting material is exposed to varying magnetic field. These losses can be reduced by using highly resistive stabilizers but it is a trade-off with the thermo-electrical dynamics and stability of the wire in case of local transition of the superconducting material into highly resistive.

Coupling losses in superconducting wires are due to mutual coupling of filaments in varying magnetic field. Filaments couple inside the conductor to prevent the change of magnetic flux through as predicted by Faraday's law. As a consequence, the induced screening currents flow from filament to another through the resistive matrix metal generating losses. Coupling losses can be reduced by twisting the conductor around its axis. The filament loops seen by magnetic flux are therefore reduced in size and thus the losses, that are proportional to the size of the loop, become smaller. [27, 50]

Hysteresis losses are related to magnetization of hard superconductors. Looking from the microscopic point of view, when the magnetic field B is greater than B_{c1} , due to strong pinning in the mixed state, the flux tubes tend to get stuck to pinning centers. Even if B is decreased back to zero, flux tubes do remain trapped and reversal field has to be applied in order to clear off all the trapped flux. In this procedure flux lines move and thus losses are generated. From the mesoscopic point of view, losses in superconductor can be described as ohmic losses that are generated in the presence of both, electric field (\mathbf{E}) and current density \mathbf{J} both having component to the same direction, where time-varying magnetic field induces electric field into the superconducting material. [27, 67]

Losses are important to take in to account when assembling different cable geometries in, to which the attention is turned next, order to ensure desired functionality and stability of cables. For example, the coupling losses are generated also in multiconductor cables, therefore twisting is a standard manufacturing technique cables.

2.3 Cables

Conductor manufacturing has typically been limited to round conductors having diameter of 1-2 mm or to wide and thin tapes of width 12 mm. In some applications high operation current is required. Since single conductors have low I_c , conductors are assembled into cables. Cables are made of superconducting wires, e.g., in order to decrease AC losses or add channels to the structure for forced cooling. AC losses are decreased typically by twisting the wires around the cable center. In AC use, the twisting is not only beneficial in reducing the coupling losses but also in homogeneous current density distribution in the cable's cross-section. Otherwise, current would flow mainly in the inner strands, e.g. in case of coils, resulting in lower performance.

2.3.1 Rutherford cable

Because LTS wires are typically round [4], it sets some requirements on the cable design. Practically the only LTS cable type, used in the accelerator magnets, is the Rutherford cable [65]. Geometry of the cable is shown in Figure 2.4, where the twisting of wires can also be seen: Every single conductor makes a full transition around the cable over the length of the twist-pitch.

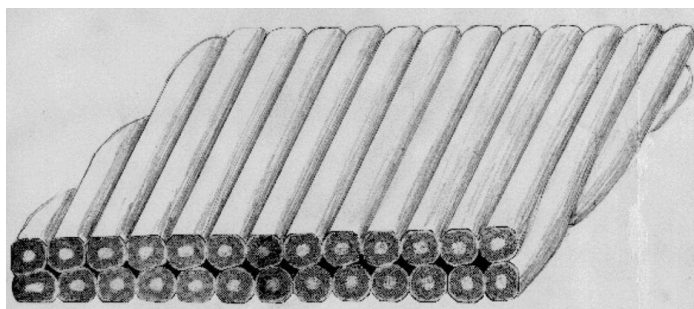


Figure 2.4. Geometry of Rutherford-cable. Figure from [65].

Twisting makes the Rutherford cables suitable for AC applications. Moreover, the rolling phase in the manufacturing makes the cables flat giving coils, made out of it, a good packing factor - thus compact size, higher energy density and therefore higher magnetic fields can be generated. The number of LTS strands in a cable is typically 30-40.

2.3.2 Cable-in-conduit conductor

Large magnet systems for fusion, however, do require different cable geometry compared to Rutherford cable for example. Since the systems like ITER [38] are typically large in size and operated with current up to 50 kA, cooling challenges arise. Also, in fusion systems rapid magnetic field change occurrence sets requirement for low coupling loss. Therefore, a special kind of cable design has been developed, namely cable-in-conduit conductor (CICC).

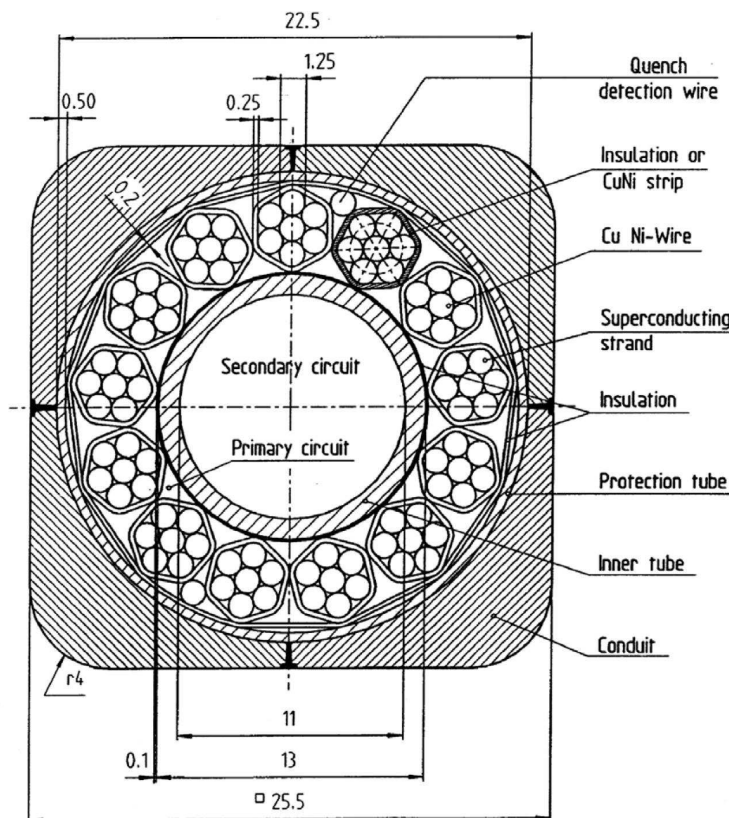


Figure 2.5. Cross-section of the POLO conductor. Figure from [24].

The cables that are used in CICC are twisted LTS strand bundles. To give an example of a CICC, the POLO conductor is presented in figure 2.5. The design resulted as an outcome of the POLO project. The objective was to design a CICC to meet the requirements of a large fusion magnet system. The main problem was the cooling due to large operating currents and AC losses induced by the rapid field changes. As a solution to the design problem, an idea of a dual cooling system was introduced and finally proven to be very functional way to cool the conductor, and thus the magnet. The dual cooling system consists of a primary and a secondary cooling circuit inside the POLO conductor. In the primary cooling circuit the coolant, Helium, is in direct contact with the superconducting cables. In the secondary circuit the coolant is forced to flow in the inner tube. [24]

2.3.3 Roebel cable

When the investigation on HTS tape applicability for cable based applications was started, Rutherford geometry was not an option. This led to a new kind of cable design: the Roebel cable. Perhaps the most promising cable type for alternating high magnetic field applications is the Roebel cable [17]. This cable geometry was developed in order to assemble HTS tapes into cables having low coupling loss and homogeneous current distribution. Special techniques are therefore needed in manufacturing, since the cable cannot be assembled by twisting as in case of Rutherford cables.

The so-called strand punching technique was originally introduced by Wilfried Goldacker [18]. In that technique, individual strands are mechanically punched from a single wide one and then assembled into a Roebel cable depicted in Figure 2.6, resulting in cross-sectional configuration as shown in Figure 2.7.

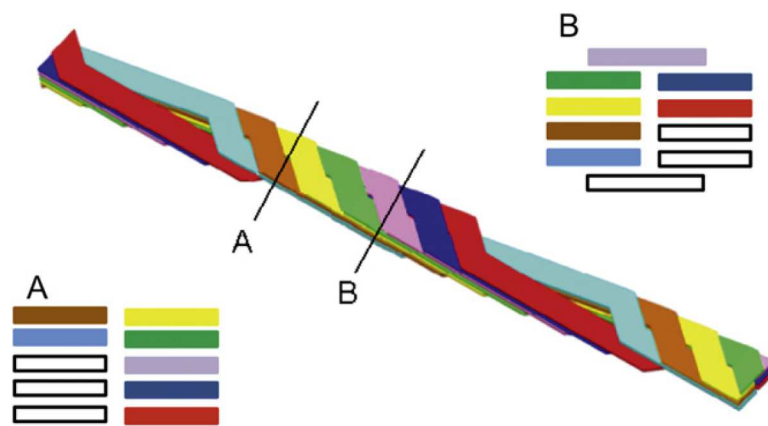


Figure 2.6. Structure of a Roebel cable. Figure from [19].

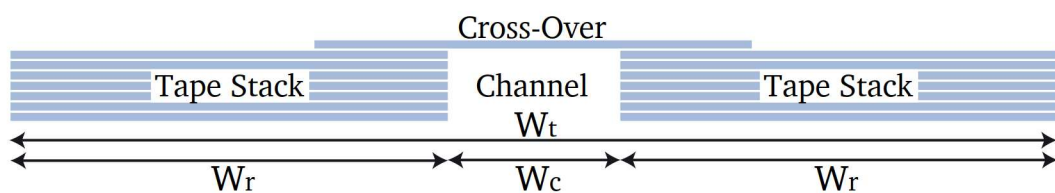


Figure 2.7. Cross-section of a 15-tape Roebel cable. Figure from [60].

The together-assembled tapes have a certain transposition length analogous to the twist pitch of conventional cables made of round wires [19]. This fabrication method is very successful and results in very stable cables: Even if one of the tapes was literally broken, the current would redistribute and go around the weak spot in the cable - thanks to low contact resistances. The downside of this production method however is the high price: When punching the individual strands, around half of the material is thrown away³. Also

³The punched off material is certainly recycled but it has to be re-manufactured since the pieces are too small to use for any application straight away.

long length cables are difficult to manufacture. In Figure 2.8 a Roebel cable ready for magnet winding is shown.



Figure 2.8. Photograph of a Roebel cable. Figure from [60].

2.3.4 Other cable developments

Another HTS cable type to be mentioned is conductor on round core (CORC). It has similar geometry as CICC's since the round core can be a hollow former allowing forced flow cooling for the cable increasing the stability of it. In the future HTS based CORCs could be used in fusion magnets thanks to their good stability in high disturbance conditions. In Figure 2.9, such a cable geometry is shown. Tapes are wound on top of each other forming layers of desired amount. Moreover, depending on the diameter of the round core, the strand width is chosen such that sufficient flexibility is enabled in order to be able to wind the tapes around a round core.[3]

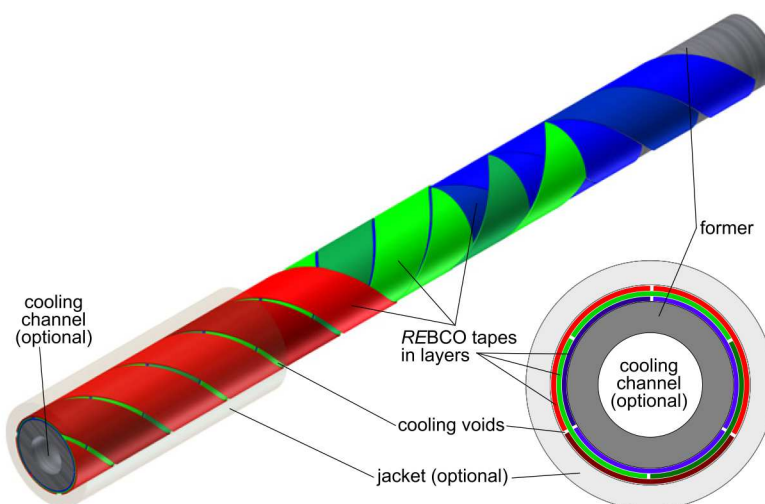


Figure 2.9. Depiction of a HTS tape based CORC cable. Figure from [3].

In Figure 2.10 one possible geometry for twisted-stack cable is shown. It has five 30-tape stacks twisted around a round core. The core of the cable is made of aluminum, in this design, providing good winding, mechanical and thermal properties. The slots, that

guide the stacks around the core, determine the twist-pitch of the cable improving AC its behaviour. The pipe in the center of the cable can be used for forced cooling. [9]

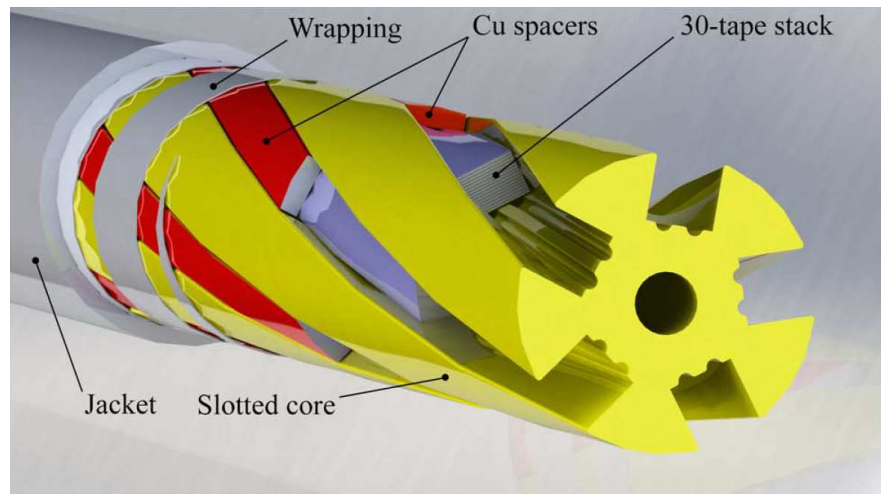


Figure 2.10. Twisted-stack cable geometry. Figure from [9].

A configuration of superconductor based 3-phase power cable is shown in Figure 2.11. Typically such cables are made of HTS tapes. This is beneficial, since liquid nitrogen can be used as coolant. Moreover since High- T_c wires can be easily manufactured in tape form, cable diameter can be kept relatively small and current densities high. Windings of each three phase are wound around a round former and insulated. Between the phase layers cooling is also provided. [20]

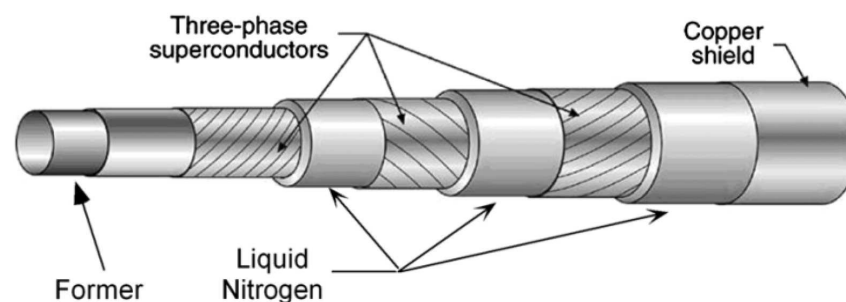


Figure 2.11. Three-phase superconducting power cable. Figure from [20].

2.4 Applications

The applications are mainly still at the state of R&D projects - magnetic resonance imaging devices not being one of those however. [50] The R&D projects can be divided into smaller and larger projects. From the big science side one could name the Large Hadron Collider in the European Organization for Nuclear Research (CERN) [10] and the fusion device project ITER [22]. In this section, an overview of different applications is given.

The majority of the applications are LTS based, the need for high-current cables has driven the focus of R&D programs to HTS based applications. The current interests are for example in wind turbine generators [39] and transmission lines [64, 68]. In wind turbines, the HTS cables in rotor winding instead of permanent magnets for example can reduce the weight of hub down to a quarter. At high powers, the use of superconductor based cables in transmission lines reduces significantly the power loss per year compared to the conventional normal conducting cables [25].

Superconducting magnetic energy storage (SMES) consists of a superconductor based coil, cryocooler and of a power conversion system. This energy storage is charged by persisting a current flowing into the coil. Since in DC use essentially no resistive losses generate, high currents and thus high energies could be stored in such devices. The advantage of SMES is that, large energies can be charged and rapidly discharged to power back-up systems. Utility applications are mainly related to stability maintenance of power grids in case of power cuts for example. [20]

In power grids, several components could be replaced by superconductor based ones. Now, investigations are ongoing on fault current limiters (FCL) [26] and transformers [72], to name some. Since superconducting cable based devices have the capabilities of high energy density, high efficiency and compact size, they are favorable for electric motors and generators also. These features are beneficial for example in future aircraft industry [33]. Moreover, in some applications very high performance from electric motor is required, in terms of torque for example, then superconducting winding is an option.

In particle colliders, like the Large Hadron Collider in the European Organization for Nuclear Research (CERN) [10], powerful magnetic fields are required for squeezing (quadrupole magnets) or for steering (dipole magnets) the beam. When reaching out for higher collision energies more magnetic force is needed to keep them in the circular orbit. In the future, in order to reveal more and more about the universe and the matter itself, higher collision energies are undoubtedly required. Thus, the use of high performance HTS cables in accelerator magnets is inevitable.

2.5 Remarks

In the chapter, starting from the basics of superconductivity, different superconducting wires were presented based on the most promising compounds. When aiming for specific applications tailored cable designs are often required to reduce AC losses or add extra cooling inside the cables like in the case of Fusion systems. Therefore it is important to know the limitations and behavior of the single wires under the desired operation conditions: Superconducting state is maintained if T , J and B are below the critical surface of the superconductor. This basic idea leads the outline of the thesis to topic of superconductor stability. The next chapter deals with the consequence considerations related to loss of superconducting state during operation of superconductor based device and how to be prepared for such undesired malfunctionality.

3. SUPERCONDUCTOR STABILITY

Superconductor stability is most of all related to maintaining the adequate operation conditions suitable for the specific device. It is therefore of the utmost importance to determine the margins to a point when stability is lost and keep the operation point below the critical surface. However, any superconducting system must have a detection and protection system in case of loss of stability due to an unexpectedly high disturbance. Otherwise the device will be damaged and repairing a superconducting system is very difficult and time consuming if even possible. In this chapter, the general concepts related to superconductor stability, with especially magnet applications in mind, are presented.

3.1 Disturbance spectrum

Disturbance spectrum represents the different sources of energy in the superconducting magnet, that can lead to loss of stability. The effect of these on the device in the operation conditions should be considered in the designing process. A disturbance spectrum for superconducting accelerator magnet is shown in Figure 3.1. It presents the energy density, as a function of disturbance time, caused by flux jump, wire motion, particle showers, AC loss, nuclear heat and heat leak. For example flux jump, wire motion or particle shower can be very short in time but still powerful events in terms of energy density that they generate. Longer period or even continuous disturbances can be AC loss, nuclear heat and heat leaks. In summary, all these must be taken into account and evaluated in order to be sure about the sufficient stability of the system in operation.

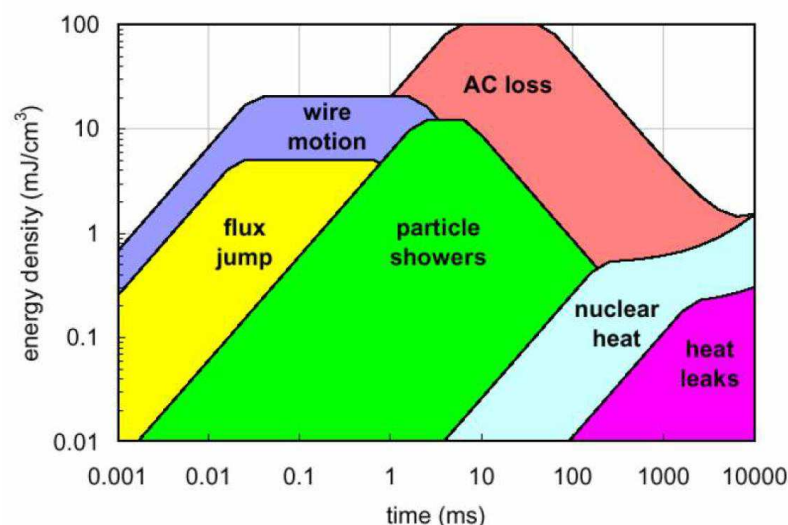


Figure 3.1. Depiction of superconductor disturbance spectrum in an accelerator magnet. Figure from [6].

In Figure 3.2, Wilson's classification of the different disturbances in space and time is shown. In time, disturbance can be either transient type of, or continuous. In space-wise division they can be point-wise, i.e. something local, or distributed, i.e. disturbance occurs in larger volume.

The transients are such disturbances that they happen only once - like in-time short energy pulse due to wire motion caused by insulation crack for example. In these cases the one is interested in the amount of released energy in Joules. On the other hand if a short energy pulse is distributed into a larger volume, then the interesting unit is Joules/m³.

Time-continuous disturbances are also divided according to the volume of occurrence. Since they are continuous, it is more relevant to measure such disturbance in Watts for point-wise and in Watts/m³ for energy generation in larger volumes. AC loss is an example of a continuous distributed disturbance.

		Space	
		<i>Point</i>	<i>Distributed</i>
Time	<i>Transient</i>	Joules	Joules/m ³
	<i>Continuous</i>	Watts	Watts/m ³

Figure 3.2. Wilson's disturbance spectrum. Figure from [66].

Disturbance, like heat generation in resistive current joint of superconducting cable, that is greater than the available cooling can cause a thermal runaway, i.e. an uncontrollable heat generation. After a disturbance that causes the superconducting winding, or a part of it, to transit into resistive state from the superconducting one, thermal runaway is highly likely. This is partially due to the fact that superconductors are often operated with high currents.

3.2 Quench

Quench is an unwanted and irreversible thermal runaway, which is due to disturbance-caused transition of superconducting material from superconducting state into highly resistive one. Consequently, possibly high operation current starts to flow in the less-resistive matrix metal resulting in heat generation. If the rate of heat generation is such that the available cooling is insufficient, like in the case of quench, the superconducting system needs to be de-energized in a proper manner in order to avoid breaking the device.

To describe quench from another point of view, in Figure 3.3 the chain reaction principle of the thermal runaway is sketched. In this model the chain of different effects, that lead to quench, are categorized and explained as follows. Due to motion of flux lines in superconductor, the flux jumping ($\Delta\phi$) caused by disturbance, heat is dissipated (ΔQ)

which leads to temperature rise (ΔT) that furthermore has directly has a negative effect on the critical current density ($-\Delta J_c$). As a consequence of the J_c decrease, more flux motion generates [21]. To notice, the chain effect can start at any point of the chain. However, if cooling is insufficient, the thermal runaway accelerates resulting rapidly in quench.

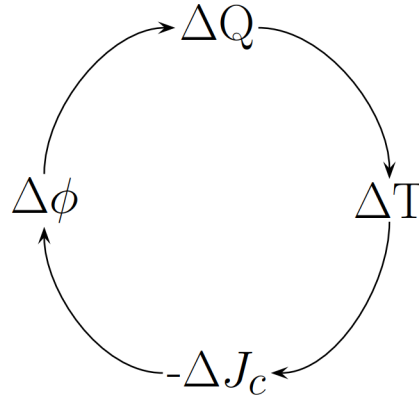


Figure 3.3. Illustration of a quench chain reaction Figure from [21].

Due to existing possibility of such thermal runaway, caused by a disturbance, the system needs to have suitable quench detection and protection. From the engineering point of view, to be prepared for a quench one needs to simulate various possible quench events before the magnet operation to be able to predict if a quench can be safely carried through. In addition, simulations are needed in designing adequate protection systems for such magnets.

3.3 Stability margins

Stability margins describe the maximum change of operation point before superconducting device quenches. Therefore it is necessary to estimate the margins in design process. These estimates are typically based on the characteristics of single conductor. Based on that, simulations are performed for the whole device under design to set the operation point such that the desired performance is obtained with reasonable stability margins. Moreover, stability margins can be divided in three: Current margin, temperature margin and enthalpy margin.

Current margin is the increase of operation current such that it reaches the critical point of the magnet, i.e. when magnet's critical current is the same as its operation current, I_{op} . Another margin to be considered is the temperature margin. This means the increase in temperature to the current sharing temperature (T_{cs}), i.e. to a value such that critical current decreases to I_{op} . Closely related to temperature margin is enthalpy margin which describes well the stability of the superconductor in terms of how sensitive it is to disturbances. Enthalpy margin is defined as the integral of heat capacity of the conductor from the operation temperature to the temperature where the critical point is reached. [52]

In Figure 3.4 magnet's load line is drawn with the operation point sliding on it as a function of operation current. The margin to quench is set by the critical current, i.e., $J_c(T, \mathbf{B})$. The higher \mathbf{B} or T gets, the smaller becomes the margin in the load line. Notice that in HTS tapes, not only the magnitude but even more strongly the direction of \mathbf{B} has significant effect on the critical current. However the described principle above is the same for HTS magnets.

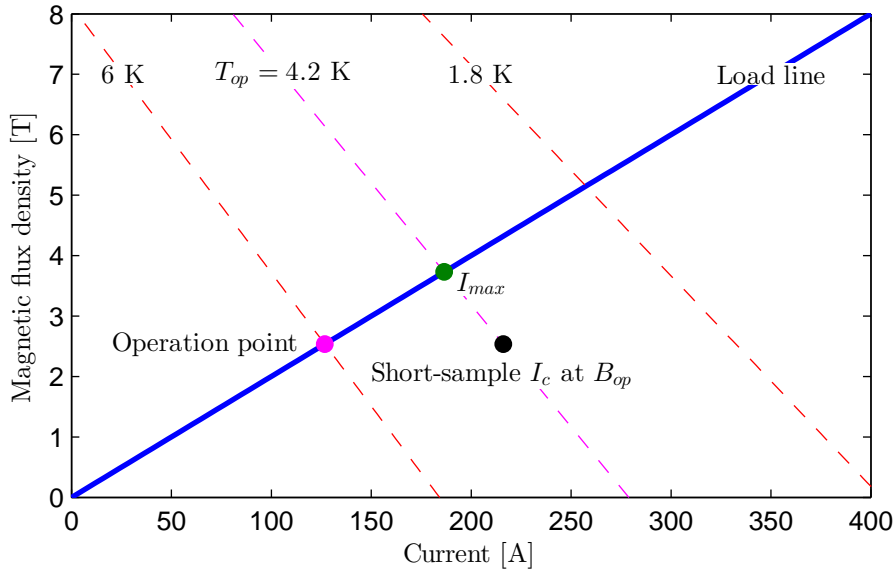


Figure 3.4. Illustration of magnet's load line (solid line) and critical current characteristics at different temperatures (dashed line).

Minimum quench energy (MQE) is often computed when estimates on stability margins are studied. MQE, in Wilson's spectrum (See Figure 3.2), would fall in to the class of point-wise transient disturbance. MQE is the amount of energy required to quench the device. Due to this disturbance the critical current density decreases below the operation point. Consequently, current is shared into the resistive stabilizer metal of the conductor resulting in joule heating. This leads to quench if the disturbance energy is greater or equal to MQE.

Another term, closely related to MQE, is the minimum propagation zone (MPZ) - the smallest normal zone volume such that the resulting heat generation leads to irreversible loss of stability. In addition, MQE is the energy required to generate MPZ. However, the normal zone is often defined as the volume in temperature above T_{cs} . However, if the volume of the normal zone is smaller than MPZ, the conductor can recover due to heat diffusing away from the zone. [52]

3.4 Quench protection

If a quench occurs in superconducting device, its protection system must be activated rapidly in order to avoid too high temperatures that can damages the structure. Quench

protection, in general, is divided in two different kinds: active and passive. Active protection relies on quench detection: When quench is detected the protection system is activated. In passive one, the system is designed in a way that it is self-protected meaning that no active quench detection or protection system activation is needed. Moreover, in case of quench, the system has to be de-energized. This can be done in two ways: transform the energy into heat either internally in the structure of the device, or externally to a resistor for example. Different developments of quench protection systems, based on the main concepts, are presented in this chapter.

3.4.1 Energy extraction with dump resistor

The energy extraction system with dump resistor is an active protection system of a superconducting magnet where the coil's energy is extracted in an external dumping resistor. The Figure 3.5 depicts the energy extraction system in terms of a circuit diagram. In case of the quench current source is switched off and coil is connected in series with a resistor (R_d). The normal zone, via which the current passes, has a resistance (R_{coil}) that changes during the quench and de-energization. The time required for the current to decay can be estimated with the time constant $\tau = \frac{R_d + R_{coil}}{L}$.¹

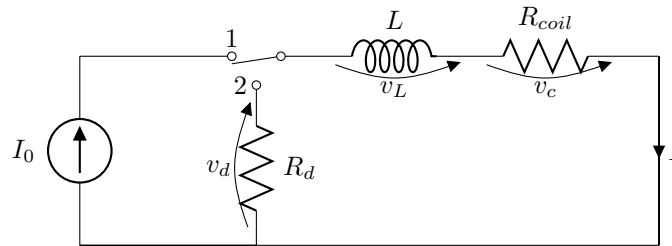


Figure 3.5. Circuit diagram of the energy extraction system.

Detection voltage is the resistive voltage of the magnet at which the quench is detected. However, to validate the quench, resistive voltage has to be above the detection voltage for certain *validation time*. When the quench is validated, the protection system is activated, within *activation delay* that the power electronics take to switch off the current source and connect the dumping resistor with the magnet.

However, large magnets cannot be protected like this [49]. Energy extraction system works sufficiently only if the normal zone resistivity is much smaller than the dumping resistor. In LTS magnets the normal zone propagates fast to all directions in the structure, thus, those kind of magnets typically have high normal zone resistance making them hard to protect using external dump resistor. However, in HTS coils the normal zone propagates very slowly, making them easy to protect with energy extraction system.

¹To note, by definition τ is the time required for the decrease from the initial value to $\frac{1}{e} \approx 37\%$ of it. In physical systems like here, the current should decrease down to $\sim 5\%$ of I_{op} to be in safe mode.

3.4.2 Protection heaters

Protection heaters are used to transfer quickly the whole magnet into normal state letting the magnet's energy transform into heat in the stabilizer. The heaters are typically made out of thin stainless steel integrated in the coil structure by gluing them into close contact with winding [44]. When quench is detected, heaters are fired using a capacitor bank. Protection heaters bring the winding into normal state initially from the efficient surface area due to heat flux from heater into the winding. The flux can be characterized by the heater surface power P_{PH} ($\frac{W}{cm^2}$), which is an important parameter in heater design [48]. The resistive volume, due to heaters, in the winding absorbs the coil's magnetic energy and prevents too high local temperatures in the structure. [48]

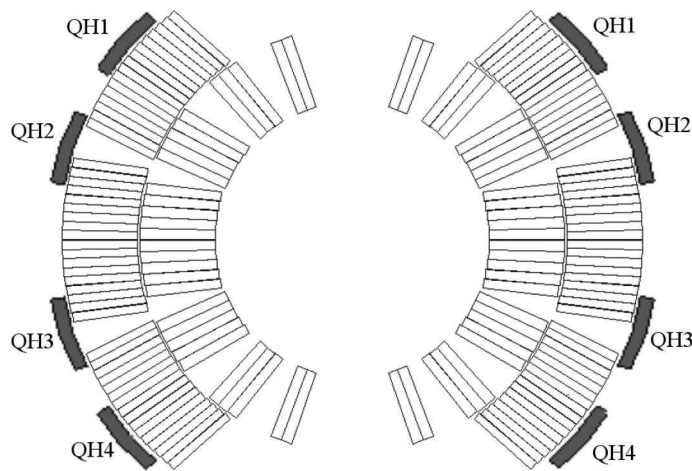


Figure 3.6. Four quench heater circuits are implemented on the LHC main dipole magnet's most outer winding layer. Figure from [44].

Quench heaters do have their limitations since the massive capacitors, needed to fast energization of the heaters, are very expensive. It has been also remarked in practice that they are not long-lasting and robust. Clearly, there is need for more advanced protection systems.

3.4.3 CLIQ

The Coupling-Loss Induced Quench [44] (CLIQ) is the most recent idea on how the LTS magnets should be protected internally. This technology relies on the coupling losses: When quench is detected and CLIQ activated, it introduces an alternating current to flow in the winding. The generated coupling losses then raise the temperature of wires by means of joule heating and finally quench the magnet. System's energy is thus transformed into heat internally, like when using protection heaters.

A circuit diagram of the CLIQ unit is presented in Figure 3.7. It consists of a power supply, a capacitor bank of several parallel capacitors and of a dump resistor (R_d) for discharging the capacitors when switching the device off.

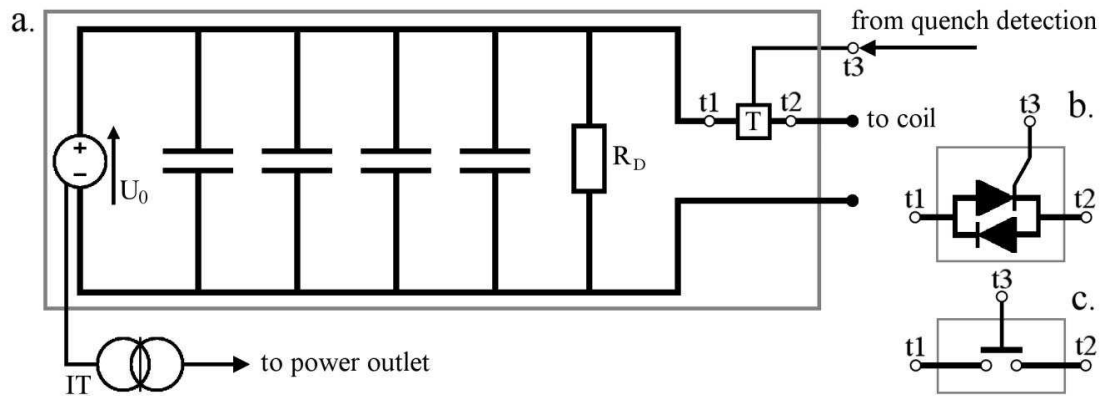


Figure 3.7. A schematic of CLIQ unit's circuit diagram (a.). The trigger box, T , can be either a diode-thyristor anti-parallel connection (b.), or an electronic switch (c.). Figure from [44].

Albeit this method works for LTS based magnets, it is not efficient enough for protecting HTS cable based magnets due to their high stability margins. A different kind of protection method is needed for those.

3.4.4 E³SPreSSO

Energy Extraction Symbiotic Protection System for Series Operation [61] (E³SPreSSO) is an active energy extraction system designed for HTS coils. A single E³SPreSSO unit (see Figure 3.8) is made of bifilar superconducting cable wound into a coil shape, therefore having low self-inductance. Moreover, the used cable could be for example NbTi based, which is relatively cheap and used also in the accelerator magnets of Large Hadron Collider.

The system works as follows. When quench is detected, E³SPreSSO is activated using a CLIQ or heaters, which makes the unit to quench and become highly resistive. Consequently magnet's current starts to flow in the parallel resistor R dissipating system's energy - in other words, E³SPreSSO works as a superconducting switch. Moreover, if the energy to be extracted is high, the magnet can be divided into several sections, each protected by such an E³SPreSSO unit. Furthermore, one of the main advantages of E³SPreSSO is that, since its connected in series with the main coil, it does not require expensive switches. [61]

3.4.5 ICED

Inductively coupled energy dissipator (ICED) is a passive protection concept to inductively extract a part of the magnet's energy in to a secondary circuit. The secondary circuit is a copper ring placed around the magnet's winding. In Figure 3.9, a circuit diagram of ICED system shown, where the loop-circuit repre-

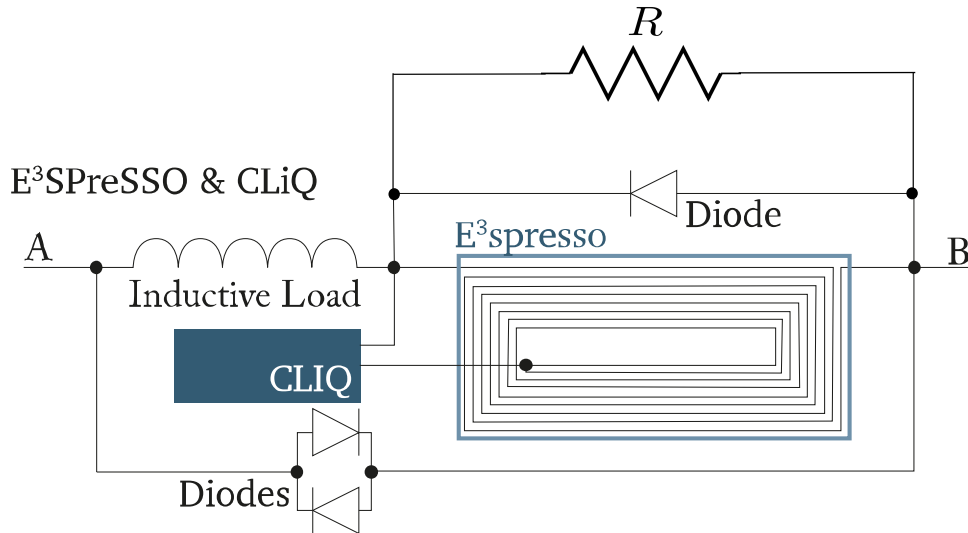


Figure 3.8. A sketch of E^3 SPreSSO unit with CLIQ-activator. Figure from [61].

sents the ICED loop. Due to rapid change in magnetic field during the after-quench de-energization of the magnet, eddy currents are induced to flow in the ICED and extracted energy is transformed into heat. [40]

This concept, however, has its downside if used with accelerator magnets: When energizing the magnet, i.e. ramping the current up, so-called loading losses are generated in the secondary winding. These losses have to be taken into account when estimating the stability margins. [40]

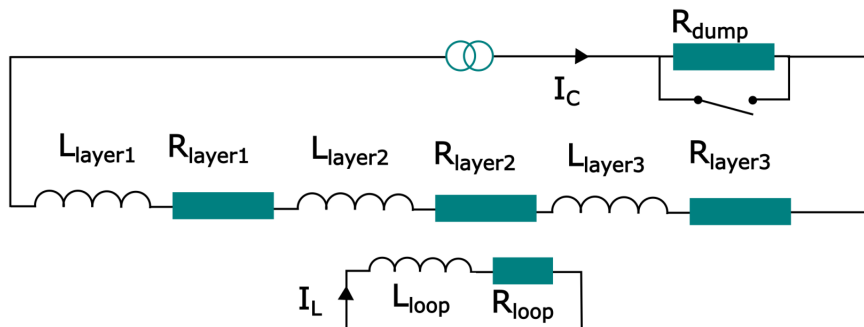


Figure 3.9. A circuit diagram illustrating the ICED concept. Figure from [40].

A similar concept has been already applied within EuCARD-2² program for Feather-M2 HTS demonstration accelerator magnet. Together with external dump resistor, it has been proven to speed up the current decay significantly resulting in lower hot spot temperatures during a quench. [23]

²Enhanced European Coordination for Accelerator Research & Development [46]

4. QUENCH MODELLING

Quench modelling is about designing a reliable quench detection- and protection system for device. In the simulations, the objective is to ensure that the device will not get damaged during quench and de-energization for any reason. Such reasons are, for example, too high temperature, too high voltage to ground or between the cable turns. The damages that too high temperature and voltage can cause are material phase transitions and electrical breakdowns, respectively. The first one can degrade the device's critical current and the second can cause an electric short for example due to electrical insulation failure. Degradation of critical current, or electrical insulation, can also occur if local stress during quench damages superconducting wire or its insulation. This can occur, for example, due to combination of Lorentz forces and local thermal expansion. Mechanical simulations can be used to estimate if there is a noteworthy risk for this. Since superconducting devices are highly expensive and difficult to build, reliable simulation methods and tools are essential in ensuring that no device breakdown occurs in case of a quench. Quench simulations can be tedious as the problem is an interplay of different areas of physics.

In this chapter, quench as a multiphysics problem is discussed. The topic is accessed by compartmentalizing the different physics that interplay in a quench event. The viewpoint is that of a modeller: Because the real world problem requires necessarily substantial simplification for simulations, the key question in the beginning is: What are the modelling decisions one can take? Furthermore the discussion proceeds via different modelling approaches to considerations on material properties, critical current density characterization and how to model heat generation in a superconducting strand or cable during a quench. At the end, before the remarks, we shortly review two numerical methods that can be used to solve partial differential equations with computers. The quench modelling tool that is presented in chapter 5 implements a combination of these two to solve heat diffusion equation in a modelling domain representing a superconducting magnet.

4.1 Quench as a multiphysics problem

The three coupled domains of physics that are involved in quench modelling are thermodynamics, electromagnetics and mechanics. How these fields of physics couple together and what one can solve with these is next presented.

Quench is first of all a severe thermal runaway inside a device. The heat diffusion and generation is modelled with thermodynamics. In a superconducting strand or cable, the heat diffusion equation governs the thermal problem. Most of the material properties, also in other physics, are temperature dependent. Without thermal modelling it is not possible

to know the maximum temperature, the hot spot temperature, during a quench. Therefore, the quench modelling necessarily includes some kind of thermal considerations.

Quench is often a fast process, after the thermal runaway has started with a steep time derivative of hot spot temperature, there is only a fraction of second to de-energize the device. Therefore, a common approach is to consider the superconducting part of the system, like the windings in a magnet, adiabatic. More profound approach, which is also sometimes necessary for reliable modelling, is to consider the heat transfer from the quenching part to the coolant. Simplest approach completely neglects heat conduction and assumes that temperature increases according to the balance of heat generation and enthalpy. This approach considers quench spreading by other means - for example by knowing normal zone propagation velocities. Other option in case of active dissipative quench protection is to know quench delays for different parts of the device. This approach models these parts isothermal and adiabatic.

Heat generation in a superconducting device depends locally on three parameters, J , \mathbf{B} and T - the same ones that define whether a given location is in normal state or not. In a magnet the J and B are solved with the models of electromagnetism. Resistivities of normal conducting constituents, such as copper, depend notably on temperature. Therefore, the electromagnetic and thermal physics are coupled.

Electromagnetic description of a quenching superconducting device is quasistatic: the decaying current excites a time varying magnetic field which induces AC-losses and influences on local current densities. On the other hand, the net currents can be modelled with circuit theory and approximation of magnetic field density at given time instant can be computed from the known net currents of the strands or cables.

Superconducting devices are very finely structured technology. Therefore it is often not possible to approach the electromagnetic physics with quasi-static field models where the modelling domain represents the superconductors at filament level. Different kind of approaches can be taken: a conservative one neglects AC-losses, assumes infinitely fast current diffusion from the quenching superconducting filaments to the stabilizer and solves magnetic flux density distribution from homogeneous current density. Even linear approach is very useful in which \mathbf{B} distribution is only solved at operation current and then scaled to other currents. With this information heat generation in the thermal part of the problem can be solved.

Current carrying superconducting device is always connected to an external circuit¹. In this circuit the stored energy of the device is modelled with inductance, which can also vary. Other important constituents of this circuit are the normal zone resistance in the magnet and possible external resistances - in addition to the current source that must be

¹Even in case of persisted magnets, where magnet is short circuited with a superconducting switch after energization, one can consider the device to have an electric circuit.

by-passed. This circuit is important for modelling current decay. Naturally, this current decay can be modelled also via energy balance: operation current determines the energy stored in magnetic field: when energy is dissipated, the current must decay correspondingly.

Mechanical design of superconducting devices is rigorous. Thermal shrinkage during the cooldown and Lorentz forces arising at energization cause a stress state to the device. The support structure and winding must be designed to withstand the caused stress state. This stress state starts to change when quench originates and some parts of the device start to expand. During current decay the influence of Lorentz forces lessens. This is how thermal physics affect on the mechanics.

Pedantically, the thermal expansion during quench has also influences on the dimensions of the winding and therefore on the heat diffusion. This forms a link from mechanics to thermodynamics making them non-decomposable [28]. However, to our best knowledge this kind of considerations have not been done in quench modelling so far. Only recently the first considerations of mechanics during quench have been done [71] and these have been carried only after the time evolution of temperature distribution is known.

In summary, quench modelling is a challenging multiphysical problem. To be able to perform simulations in reasonable time-frame with sufficient accuracy, simplifications, i.e. modelling decisions, has to be done.

4.1.1 Modelling decisions

Modelling decisions are taken when approaching the quench modelling problem computationally. Clearly, solving the presented physics with time-dependent field models in a 3-D modelling domain representing the superconducting device at filament level is often not reasonable. Therefore, one searches for appropriate approach for given situation where the representation of the modelling domain is practically simplified and essential physical phenomena are considered. This also sets a research direction on quench modelling methodology. According to our current understanding, different quench problematics require different approaches and there is no tool that can tackle all the quench related problems - especially when we constraint the computation time.

When one makes modelling decisions where physics is simplified one should do conservative choices to be sure that if the results predicts safe quench, real world quenching is safe. However, two conservative choices can prevent some technological advancements. Therefore, well reasoned modelling decisions are important in engineering work.

In thermodynamics simplifications can be done on the adiabaticity of the system. This is related to cooling - whether it should be taken into account or not. The answer for this one can be found by considering the ratio of cooling and heat generation during the quench. In addition this is related to the time-frame during which the quench occurs. To

give an example, if there is heat generation in large relative volumes in the system for long period of time, and the cooling is efficient, then one should take the cooling into account. Typically in quench analysis, the rate of heat generation is much higher than the cooling and events are fast. Therefore, adiabatic assumption is an adequate decision to make, resulting in accurate enough predictions.

In mechanics, when estimating the forces that occur during the quench and de-energization, estimations can be done on strain- J_c dependency. Without exception, the effects of strain on J_c are not formulated in to the problem to be solved simultaneously with the heat transfer. Otherwise, the problem would become too heavy to be solved in reasonable time frame. Therefore, mechanical analysis is done in the post-processing phase.

Modelling decisions related to simplifying the modelling domain often reduce the dimensions of the modelling domain or consider some parts of the device isothermal. For example, when always almost complete turn in a magnet quench simultaneously (for example with CLIQ or heaters based protection), it is justified to do 2-D modelling. On the other hand, the cross-section of a winding consists of metal-composite superconductors insulated with a material having low thermal conductivity. Therefore, in a magnet made from superconducting cables, it can be rational to consider each strand, or cable, isothermal and just model the heat conduction along the cables and from cable to cable through the insulation. Moreover, in a simplified hot spot temperature simulation it is modelled adiabatic. Then, the hot spot temperature can be directly computed after knowing the current decay curve.

One important aspect in modelling which has simplifications is the comparison of secondary quantities to experimental data. These quantities are something that cannot be directly measured but which can be approximated with the model when some other quantities are modelled with good accuracy. For example, it is difficult to measure the hot spot temperature, but measuring current decay curve is easy. Then, if one relates the current decay curve to the adiabatic hot spot temperature on the model, one should not expect it necessarily to reflect the real world hot spot temperature very well, even if the measured and simulated current decays match well. To be precise, this kind of a modelling, assuming that material properties and model for heat generation are reliable, gives the upper limit for the hot spot temperature.

One should not expect it necessarily to reflect the real world hot spot temperature very well, even if the measured and simulated current decays match well.

4.2 Approaches to model quench propagation

Thermal problem in a quench simulation is very special: there is a propagating normal zone. Therefore, whereas general heat diffusion problems require solving for heat diffusion equation, different kind of approaches in quench modelling can be taken. For the first one we introduce how to solve the heat diffusion equation, for the second one we consider

so-called tabular approaches. In the latter approaches the spreading of normal zone is not governed by thermal conduction but by normal zone propagation due to known normal zone propagation velocities or due to known external excitation that causes parts of the device to quench. In both of these approaches models used for heat generation, presented last in this section, are the same.

4.2.1 Solving heat diffusion equation

The primary quantity to be solved, when modelling quench phenomenon, is the temperature as a function of time over the modelling domain. The solution of the parabolic partial differential equation

$$C(T) \frac{\partial T}{\partial t} = \nabla \cdot \lambda(T) \nabla T + Q(T, \mathbf{B}), \quad (4.1)$$

based on the law of conservation of energy, gives the desired predictions on system's behavior in time. The equation consists of different terms that all together describe the dynamics of the system. The left hand side represents how the thermal energy is stored into the system, where C is volumetric heat capacity. The first term on the right hand side of the equation, where λ is the thermal conductivity, represents heat propagation in the system. The second term on the right (Q) is the heat generation term that in quench modelling is typically the joule heating. Furthermore the equation is solved by discretizing it according to the chosen numerical method. [21]

4.2.2 Tabular approach

Tabular methods are based on the normal zone propagation - like the one presented by Wilson in [66]. Idea is to compute the normal zone volume evolution using the estimates on normal zone propagation velocities in different directions [66]. Temporal discretization determines the increase of the volume during each time step. The increase of volume is an isothermal shell or a layer on top of the volume already in normal zone. These shells are adiabatic and temperature evolution is approximated using

$$C \frac{\Delta T}{\Delta t} = \rho J^2.$$

In Figure 4.1 the normal zone growth in different directions is illustrated. Moreover, detailed derivation of the formulae for normal zone propagation velocities, in different directions, are presented for example in [54].

4.2.3 Heat generation

The heat generation in superconductor based devices, during a quench, is due to operation current flow in the resistive matrix metal. Different models for the current sharing from the superconducting material to the stabilizer have been developed. Two models are of particular interest: the current sharing model and the power-law model.

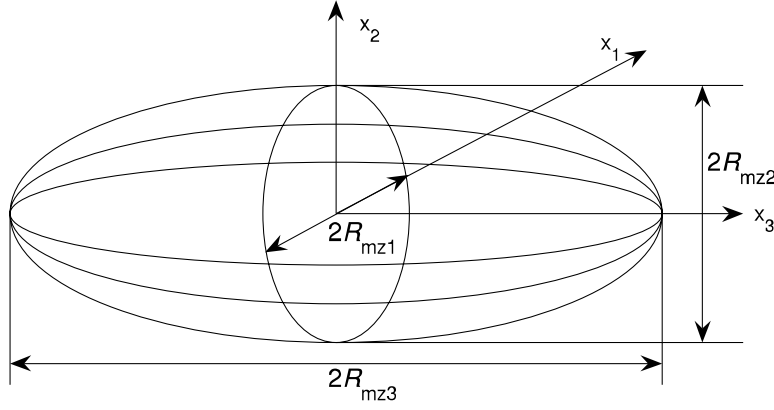


Figure 4.1. Normal zone in Wilson's method is an ellipsoidal, growing into direction of all the three radii of the ellipsoidal.

When a superconductor quenches, the superconducting region of the tape is not able to carry all the current anymore. As a function of temperature this capacity drops gradually to 0. Heat generation models describe how heat is generated in the intermediate state when the superconductor is able to carry the total operation current only partially.

Wilson's current sharing model

Wilson's current sharing model describes the heat generation by estimating the amount of current flowing in the stabilizer due to I_c -decrease as a function of T . It is simplified version of the power-law based one: It does not take into account magneto-resistivity or magnetic field dependent J_c . [66] For some rough estimates these are sufficient assumptions.

However, the heat generation per unit volume (Q) is computed as

$$Q = fJE = \frac{f^2 J \rho_{stab} [J - J_c(T)]}{1 - f},$$

where ρ_{stab} is the stabilizer resistivity, f the fraction of the superconducting material in the composite, and J is the operation current divided by the composite's total cross-section area. Furthermore, by assuming that the critical current density in the superconductor (J_c) depends linearly on the temperature such as

$$J_c(T) = J_{c0} \frac{T_c - T}{T_c - T_0},$$

where T_0 is the initial temperature at which $J_c = J_{c0}$, T_c being the critical temperature. Now, combining these two equations one gets for the heat generation

$$Q(T) = \frac{f^2 J \rho_{stab}}{1 - f} \left(J - J_{c0} \frac{T_c - T}{T_c - T_0} \right). \quad (4.2)$$

Power-law current sharing model

The current-voltage measurements based power-law can be used to describe $E - J$ relation in superconductor [8]. In its general form the power-law for a superconducting wire is

$$E = E_c \left(\frac{I_{sc}}{I_c(T, \mathbf{B})} \right)^n. \quad (4.3)$$

where E is the electric field in the superconductor, and I_{sc} is the current in the superconducting fraction of the wire. The electric field criterion E_c is the electric field in the superconductor, when J_c , determining the critical current I_c , is applied. Moreover, the exponent n characterizes how steeply the voltage depends on the current.² Typically used value for E_c is $10 \mu\text{V/m}$. Depending on the material, n -value is in between 30 and 100. For LTS high n -values are typical.

The stabilizer current I_{stab} can be solved based on the fact that the electric field is the same in the stabilizer and in the superconducting material. Then by knowing the power-law for the superconductor, material properties of the stabilizer and dimensions of the wire, stabilizer current using Ohm's law ($E = \rho J$) is

$$I_{stab} = A_{stab} \frac{E_c}{\rho_{stab}(T, B)} \left(\frac{I_{sc}}{I_c(T, \mathbf{B})} \right)^n, \quad (4.4)$$

where stabilizer's resistivity (ρ_{stab}) can magneto-resistive material. The power dissipation per unite volume in the stabilizer thus is

$$Q = \rho_{stab}(T, B) \left(\frac{I_{stab}(T, \mathbf{B})}{A_{stab}} \right)^2. \quad (4.5)$$

Quench initiation

According to the idea of disturbance spectrum, there is always some kind of initial trigger for the quench. To model quench one needs some kind of a trigger too. Setting this trigger is called quench initiation. In quench modelling, there are various ways how to initiate the quench to study the heat propagation and maximum temperature evolution during the quench and de-energization of the device. Based on research done in [21], an adequate way to trigger a quench is to set low J_c into a small area of the magnet. When operating the magnet, heat generation will occur in that area according to the used current sharing model and thermal dynamics during the quench can then be investigated. The J_c degradation in the quench initiation area can be scaled down such that the operation point is sufficiently higher in the loadline than the critical point.

²To obtain more accuracy, $n - B$ dependency can be considered. However, in this work constant n is utilized.

4.3 Material properties

In the thermal problem the material properties in question are heat capacity, thermal conductivity and electrical resistivity, which is needed in the heat generation. However, as presented, it is not possible to represent the modelling domain with all the fine details. Therefore, one needs to model the material properties for the surrogate domains based on how they are constructed. This means computing the effective material properties.

4.3.1 Effective material properties

Effective material properties homogenize a material composite to one. They are useful when the dimension of the modelling domain is reduced or some parts are assumed to be in homogeneous temperature. They give conservative estimations on how the composite would behave in reality, yet with sufficient accuracy.

The effective material parameters, volumetric heat capacity C_{eff} , thermal conductivity λ_{eff} and electrical resistivity ρ_{eff} are

$$C_{eff}(T) = \sum_{i=1}^N f_i C_i(T) \quad (4.6)$$

$$\lambda_{eff}(T) = \sum_{i=1}^N f_i \lambda_i(T) \quad (4.7)$$

$$\frac{1}{\rho_{eff}(T, B)} = \sum_{i=1}^N \frac{f_i}{\rho_i(T, B)}, \quad (4.8)$$

where N is the number of materials in the composite, T is the temperature and B is the norm of magnetic flux density. Coefficients f_i correspond to the material fractions of each material in the composite such that $\sum_{i=1}^N f_i = 1$. [54]

The derivation of the formulae is presented in [30]. The computation of effective heat capacity is based on average heat capacity per unite volume according to the different materials and their fractions. The Equation (4.7) is derived for parallel connected materials in the conductor or cable, thus representing the effective thermal conductivity along the cable. Computation of λ_{eff} is analogous to calculating total conductance of in parallel connected conductances. In Equation (4.8), effective electrical resistivity of parallel connected materials is presented - the situation is similar as in circuit theory in case of in parallel connected resistors. To note, the effective thermal conductivity in case of in series connected materials would be

$$\frac{1}{\lambda_{eff}(T)} = \sum_{i=1}^N \frac{f_i}{\lambda_i(T)}. \quad (4.9)$$

4.3.2 Representing the critical surface

In order to maintain superconducting state, not only magnetic field and temperature have to be below their critical values (B_c and T_c), but simultaneously current density in the superconductor must not exceed the so-called critical current density (J_c). From the point of view of large scale superconductor based applications, the most important thing is lossless high direct current carrying ability. To characterize the superconducting state in a practical way, fits based on measurements are utilized. It is of the utmost importance to be able to predict, how much current a superconductor can carry in certain temperature (T) and magnetic field (\mathbf{B}). Thus, here, the characterization of superconducting state is done for J_c , as a function of T and \mathbf{B} . Characterizations on critical current density are done by measuring resistive voltage over the sample at chosen temperature and applied magnetic field by increasing the transport current. Critical current (I_c) is determined with certain voltage criterion and J_c can then be scaled from that based on the stabilizer-superconducting ratio of the sample. Moreover J_c characterization for superconducting wires as a function of applied force can be done also - this is needed for mechanical modelling of superconducting devices.

Heat generation models require knowledge of critical current at operation conditions. Characterising this $I_c(T, \mathbf{B})$ surface for the range required in quench simulations is a time consuming procedure and requires special measurement setups that not all the laboratories have. Therefore, it is of special interest to develop scaling laws, or fits, for superconductors that can be tuned with only few measurement points for given conductor and that then reliably extend to a large range of \mathbf{B} and T .

The fits are well established for LTS materials NbTi and Nb₃Sn. Examples of these are the Bottura fit [7] for NbTi and the Godeke fit [16] for Nb₃Sn. As explained HTS materials are completely different, especially REBCO coated conductors, in which J_c depends also on the direction of \mathbf{B} . The optimal manufacturing processes for given applications are not known and still the performance of commercial products change from batch to another. Also, the temperature range for the critical surface is much more broad than in case of LTS and small changes manufacturing influence on the behavior differently at different temperature and field ranges. Therefore, reliable and commonly accepted fits that could characterize the critical surface of a given HTS wire have not yet been found. Naturally, several case by case fits have been done.

Figure 4.2 shows a normalized critical current surface for a NbTi conductor according to Bottura fit. Figure 4.3 describes the anisotropy in the critical current of a YBCO tape with respect to magnetic flux density according to the fit presented in [12].

However, from the electromagnetic point of view the limits of superconducting state can be described by a critical surface shown for one temperature in Figure 4.3 for HTS, i.e., if the operation point (J, T, \mathbf{B}) is above the critical surface, superconductivity is lost. In the figure, due to crystal structure of practical HTS and also due to the tape geometry, the

direction of magnetic field has a great effect on the critical current density that the conductor can carry: If the direction (θ) of the magnetic field is perpendicular with respect to the wide face of the HTS tape ($\theta=90$ in the Figure 4.3), then J_c is much smaller than in the parallel orientation. As the temperature gets higher the form of the surface stays in the same form but values for J_c become lower. [12] For round shape practical superconductors, like most of the LTS, the direction of the field has no influence in practice.

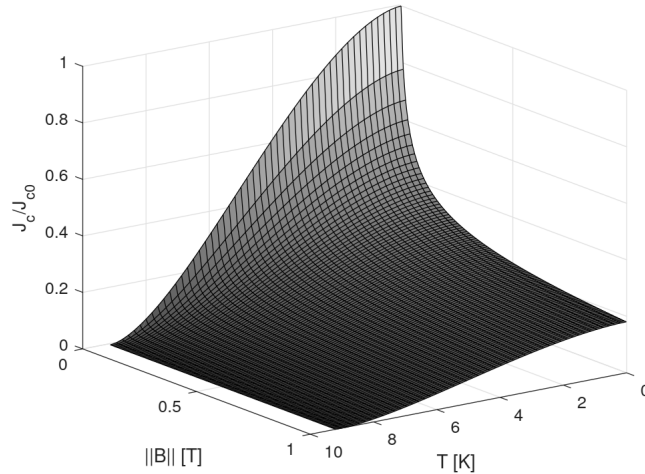


Figure 4.2. Critical surface of NbTi as a function of normalized critical current density, temperature and applied magnetic field. Fit from [7].

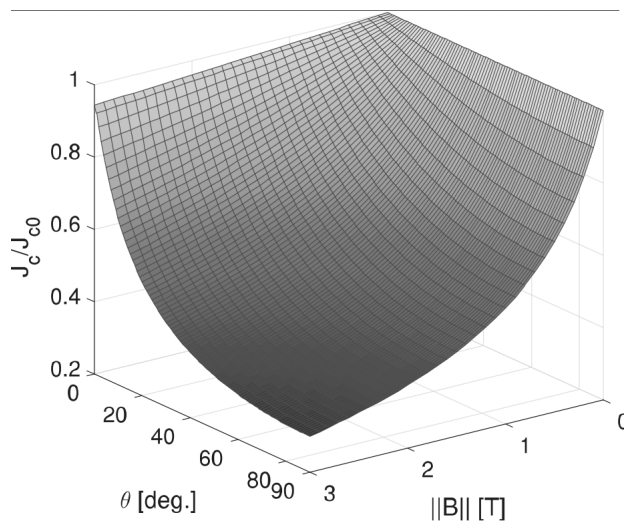


Figure 4.3. The critical current density of YBCO is highly dependent on the direction of the magnetic field.

4.4 Numerical methods

To solve partial differential equations with computers, like the heat diffusion equation, one needs numerical methods. Next two of them are presented: Finite element method (FEM) and finite difference method (FDM). The main difference between these two is that in FEM as a solution one gets the basis functions that satisfy the given equation with

given boundary conditions, and in FDM one gets directly the point-wise solution. The purpose of these methods is to represent spatial derivatives of partial differential equations with algebraic equations. Furthermore, time derivation is left for numerical methods that solve initial value problems (IVP) of ordinary differential equations. Solvers for IVPs are implemented in Matlab [34] for example. To name one of the open-source ones, SUNDIALS [56] is commonly utilized.

4.4.1 Finite element method

The finite element method (FEM) is a powerful computational technique. FEM is a numerical method for solving physical problems arising for example from the fields of engineering and applied science. The basic idea behind FEM is to represent the field to be solved as a sum of basis functions set according to discretization of the modelling domain into finite elements, adequate for the dimension of the domain.

Taking the heat diffusion problem, as an example, the solution is approximated in the modelling domain Ω using

$$T(\mathbf{r}) = \sum_{i=1}^N T_i \psi_i(\mathbf{r}),$$

where \mathbf{r} is a point in Ω , ψ_i are the basis functions and N is the number of *element nodes*. T_i are the unknown coefficients, *degrees of freedom* (DoFs), representing the temperature at element nodes i .

Via the *weak formulation* procedure, detailed in [45, 55], an algebraic system of equations is obtained, which can be presented in matrix form as

$$\mathbf{M}\dot{\mathbf{T}} = \mathbf{K}\mathbf{T} + \mathbf{Q}, \quad (4.10)$$

where \mathbf{M} is the mass matrix, \mathbf{K} the stiffness matrix and \mathbf{Q} the load vector - they represent in discretized form, respectively, the heat storage, heat transfer and heat generation. Moreover, \mathbf{T} is the vector containing all the unknown coefficients of the basis functions in Ω :

$$\mathbf{T} = [T_1, T_2, \dots, T_N]^T,$$

where N is the number of DoFs. Finally, $\dot{\mathbf{T}}$ denotes the time derivative of \mathbf{T} . [21, 27, 45]

This is the numerical method used for solving the heat diffusion equation in the upcoming simulations.

4.4.2 Finite difference method

The finite-difference method (FDM) bases on solving the unknown field at points of regular grid set over the modelling domain. The regular grid permits to approximate first- and second order spatial derivatives using Taylor series expansion. Then, an algebraic system

of equations is then obtained for each grid point and by solving it, one gets the solution at those points. [43]

Next, an example is given of a first order spatial forward difference of temperature T in two-dimensional grid of the modelling domain, shown in Figure 4.4, from grid point (i, j) to $(i, j + 1)$ having finite differences Δx and Δy in x - and y directions, respectively.

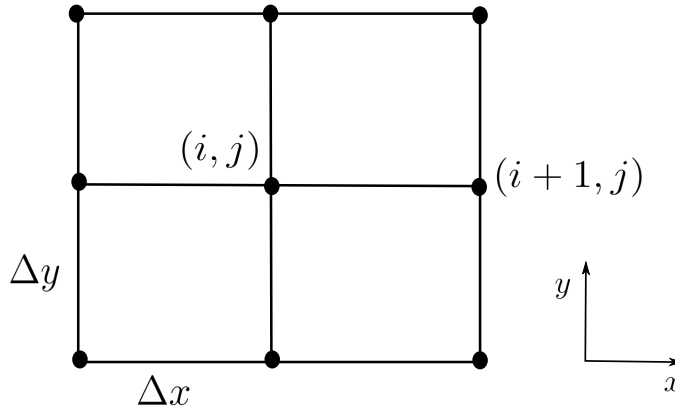


Figure 4.4. Two-dimensional discretization for FDM.

Using the Taylor series expansion [43, p. 10] and taking the terms up to the first order derivate, one gets for the derivate into x direction at (x_i, y_j)

$$\frac{\partial T(x_i, y_j)}{\partial x} \approx \frac{T_{i+1, j} - T_{i, j}}{\Delta x},$$

where Δx is the distance between points $i + 1, j$ and i, j . Here a forward difference is utilized, but backward difference and dentral difference can also be utilized. However, similarly the derivative approximations are done into other directions and higher order derivates can be recursively derived from the first order ones. Finally, as in FEM-formulation, a large algebraic system of equations is obtained and solved numerically using numerical time-stepping methods. [21, 43]

4.5 Remarks

Quench simulation tools, based on certain modelling decisions determined by the simulation case, are always compromises between accuracy and simulation time. Material properties play important role in quench simulations. The only way is to use interpolation functions, fits, based on measurements to describe their behavior in different circumstances. Moreover, two different simulation approaches are typically used when predicting heat propagation during a quench: Tabular method based one and numerically solving the heat diffusion equation (4.1), using chosen numerical method.

From now on we focus on solving the heat diffusion equation and consider electromagnetism only with external circuit and magnetic flux density distribution computed from net currents. This neglects the enhancement of quench propagation resulting from AC-losses and all the considerations of mechanics.

5. THE QUENCH SIMULATION TOOL

In this thesis work a new quench simulation tool was developed. This tool aims on new kind of 3-D modelling of heat transfer in a superconducting winding. The tool approximates the cross-section of the cable as isothermal and solves heat conduction along the cable, or strand, in a 1-D mesh. The heat transfer from cable to cable via electrical insulation is represented using finite differences based on Fourier's law [45]. The tool implements also a possibility to connect the winding to an external circuit, and therefore, model the current decay simultaneously to the heat balance.

This tool is built in Matlab on top of an open-source framework discrete problem, *dp* [53] which mainly abstracts some of the mesh facilities of open source pre- and post-processor of boundary value problems, Gmsh [14] and provides a way to pose boundary value problems in Matlab.

This chapter acts like a backbone of the tool explaining what kind of modelling decisions were taken to implement the tool. We detail these from the modelling domain and physics point-of-view. The tool takes into account more than it solves for, therefore some of the already solved data must be provided as inputs. We detail also this. We start from the physics and modelling decisions, then go to the developed numerical method for solving the 3-D heat diffusion equation by using only 1-D mesh. Finally, before the remarks, we consider the input data of the tool

5.1 Included physics and modelling decisions

This tool considers heat transfer by assuming isothermal strands or cable cross-sections. The heat generation is therefore governed by the division of current between the stabilizer and the superconducting region. Consequently, AC losses of any kind are not considered via field models and current diffusion process is not modelled. Local critical current is computed from the known magnetic flux density distribution and by integration J_c on the conductor's cross-section. User can provide any heat generation model that depends on I , I_c , \mathbf{B} and T . Further, the boundary of the modelling domain is adiabatic.

Mechanical considerations are not included, but the solved temperature evolution can be imported into a tool suitable for this. The current implementation allows only protection with external dump resistor that can be set to the magnet's circuit. However, the modelling domain can be divided into parts and own heat generation model can be given to each of them. Therefore, for example, it is possible to manually set quenching delays to different domains. This can be used to model, e.g., the heater delay - i.e. how much does it take from a quench protection heater to quench a region underneath it in a winding.

5.2 Computational approach and numerical method

The approach in this work is to solve numerically the equation (4.1) in magnet by reducing the dimension of the modelling domain from three to one. To model temperature distribution along the cable only in 1-D is based on isothermal temperature in cable's cross-section. This is an adequate modelling decision since the cross-section of the cable is small having large fraction of high thermal conductivity. Even if the computations are performed in one-dimensional modelling domain, the heat transfer between the cables is taken into account by using the FEM-FDM hybrid method, developed here and next presented.

5.2.1 FEM-FDM hybrid method

The FEM-FDM hybrid method is based on idea to discretize the whole 3-D domain using two different methods and create an one-dimensional mesh. FEM is utilized discretize and solve the heat propagation along the cable. FDM comes in to play when the heat transfer between the cable turns is formulated and discretized. The obtained system of differential equations is then added to the one obtained using FEM.

The basic idea of the FEM-FDM discretization is illustrated in Figure 5.1. The three lines represent three cable turns.¹ The elements e correspond to the ones of the FEM-discretized 1-D modelling domain.

The FEM's basis functions approximate the temperature distribution along the cable in the magnet according to the elements' nodal values, the DoFs. Then, the heat flux to e_i , from cable turns next to it, can be expressed in form of finite differences of Fourier's law, as

$$\begin{aligned} q_i &= q_{mn} + q_{jk} \\ &= -\lambda_i \frac{T_i - T_{mn}}{\Delta r} - \lambda_i \frac{T_i - T_{jk}}{\Delta r}, \end{aligned} \quad (5.1)$$

where T_i is the function that approximates the temperature in e_i . Similarly T_{mn} and T_{jk} approximate the temperature along the length of the domain, adjacent to e_i in elements m, n, j and k . Moreover, λ is the thermal conductivity of the insulation material between the turns and Δr the thickness of it. The heat flux is expressed similarly for each element and then integrated over it to obtain the energy transfer. The resulting system of equations can be expressed in form of $D\mathbf{T}$, where \mathbf{T} consists of the very same DoFs obtained from the FEM formulation. To get the units of this term consistent with the ones in (4.10), the matrix D is divided by A/p , where A is the cross-section area of the cable and p the wetted perimeter. In this case, p is the width of the cable. Now, the two systems of differential

¹For simplicity the cable turns are in one plane. Despite that, cable turns can be next- and on top of each other - the discretization principle is the same in any case.

equations are combined as

$$\mathbf{MT} = (\mathbf{K} + \mathbf{D})\mathbf{T} + \mathbf{Q}. \quad (5.2)$$

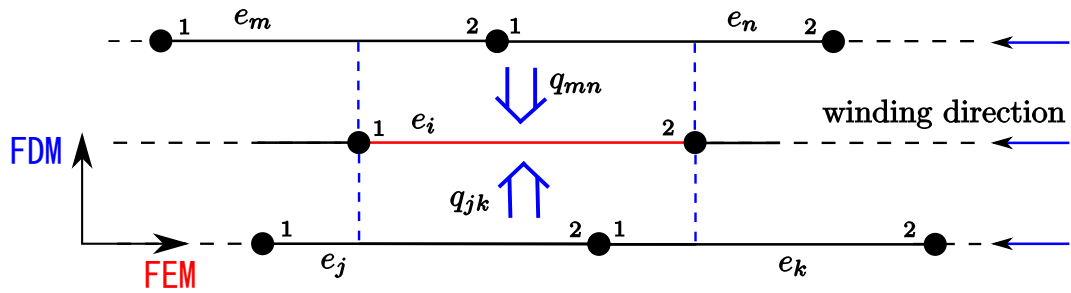


Figure 5.1. Sketch of the spatial discretization into both directions of heat flux for the two different numerical methods: Turn-to-turn (for FDM) and along the cable (for FEM).

5.2.2 Inputs

The inputs that the simulation tool needs are magnetic flux density distribution and fits describing material properties and the critical current density. Furthermore, by default, the heat generation is described by the power-law current sharing model (4.5) - however, other models for heat generation can be easily implemented and utilized.

Magnetic flux density distribution

In this simulation tool the magnetic flux density distribution, \mathbf{B} , in the modelling domain, has to be computed externally² and then used as an input. The reason behind is the assumption on linear $\mathbf{B} - I$ relation - in the simulations magnetic field scales according to the magnet current. However, if the system contains large amounts of ferromagnetic materials, then \mathbf{B} should be solved simultaneously with the heat diffusion equation.

Moreover, \mathbf{B} is required for the field dependent material properties and critical current density. It includes the information about direction of the field - this is essential if the magnet to be modelled is for example Roebel cable based.

Material parameters and J_c characterization

Since the simulations are performed using one dimensional modelling domain, material properties of the cable, consisting of several different materials, are considered as effective (See chapter 4.3.1).

Critical current wise, to put it into something practical for the 1-D modelling domain, I_c has to be computed. To do this, $J_c(T, \mathbf{B})$ is integrated over the cross section of the cable in the

²Here we have utilized a software detailed in [62].

magnet. This can be done by computing the J_c in certain amount of points in the cable's cross-section along the whole length of the magnet's cable. Here 12 sample points for I_c averaging is used. Eventually I_c is a function of T and I because it scales the magnitude of \mathbf{B} that I_c depends on - the direction of \mathbf{B} remains independent of the magnitude.

5.3 Remarks

The simulation tool was presented starting from the included physics and the modelling decisions behind the problem formulation. The new kind of approach was presented to perform quench simulations in one-dimensional modelling domain, and still taking into account the 3-D effects like the turn-to-turn heat transfer. Moreover, the functionality of the simulation tool, and required inputs, were described.

6. PREDICTING HEAT PROPAGATION IN FEATHER-M0

To develop particle accelerator magnets beyond the current state-of-the-art, new technological solutions are needed. Four years ago an European project, EuCARD-2, started whose one aim is to conduct R&D on REBCO based accelerator technology [46, 47]. One deliverable in this project was set to produce a 10 kA class particle accelerator magnet producing 5 T. To develop such technology a systematic study on smaller prototype magnets has been conducted. These magnets are called Feather-M0.x (FM0), where x identifies the particular prototype¹

In this chapter we perform quench simulations for the baseline of FM0 series utilizing the simulation tool presented in chapter 5. This is covered by description of the modelling scenario, the analysis of reference case and two parametric studies. The first investigates the magnet's critical current as a function of operation temperature. In the second one, the effect of quench detection voltage and quench protection activation delay on hot spot temperature is simulated. Moreover, due to the small size of the magnet, it is protected only with an external dump resistor.

6.1 Description of FM0 and quench modelling case

Here we present the modelling domain, the material properties, heat generation model and protection of the magnet.

6.1.1 Modelling domain

The Feather-M0.5 under investigation here has four turns of Roebel consisting of 15 REBCO tapes. The cable with insulation has width of 12.2 mm and thickness of 1 mm. A 3-D depiction of the FM0 is shown in Figure 6.1. The length of the magnet is 44 cm and width ~ 5 cm. Moreover, the inductance of the magnet is 8.16 μH .

¹From the FM0 series, so far one has been built, Feather-M0.4, but it suffered from e.g. heat generation at the current terminal and premature quenching. However, different things were learned in the manufacturing. Now, next prototype from 0-series has been build, the FM0.5 under investigation is this work, and it will be tested during summer 2017. It will be interesting to compare the measurements against the simulation results of this work.

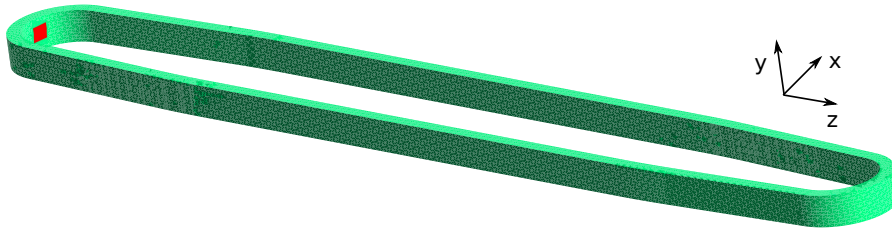


Figure 6.1. Three dimensional depiction of the magnet under study. The quench initiation point is marked at the end of the coil into the innermost cable turn.

6.1.2 Material properties

The Roebel cable consists of materials with certain fractions with respect to the whole cable, listed in Table 6.1. According to the fractions, the effective material properties were calculated based on material property fits. Material properties were taken from material library CryoComp [11].

Moreover insulation material between the cable turns is G10 fibre glass having thickness of $250 \mu\text{m}$. A J_c fit presented in [12] was utilized (The critical surface is shown in Figure 4.3).

Table 6.1. Material fractions of the Roebel cable

Material	fraction [%]
Silver	1.3
Hastelloy	36.6
REBCO	0.7
Copper	14.6
G10 & Epoxy	46.8

6.1.3 Heat generation

As the heat generation model the use the power-law based current sharing model with $E_c = 10 \mu\text{V/m}$ and $n = 30$. The quench was initiated using zero J_c in 4 mm long section of the cable. Moreover the quench was initiated, in all of the upcoming simulations, from the innermost cable turn at the end of the coil. In this location the coil has its lowest critical current because the perpendicular field component on the cable is on average slightly higher than on the straight part of the magnet. This is the most likely place for the quench in operation.

6.1.4 Quench protection

For the small prototype magnet under study, the charged energy is low enough, $\sim 580 \text{ J}$ at 12 kA, so that it can be protected using only a dump resistor, i.e., the quench protection system used to de-energize the coil under investigation is the energy extraction system

Table 6.2. Simulation parameters

Parameter	Value
Inductance	8.16 μH
Protection resistance	80 $\text{m}\Omega$
Detection voltage	100 mV
Protection delay	30 ms
Operation current	6 kA
Operation temperature	4.2 K
Hot spot I_c	0
Hot spot length	4 mm

with dump resistor. The circuit model shown in Figure 3.5 applies here as well. The value for dump resistor is determined using material based 1 kV voltage limit. An HTS magnet can be protected with a dump resistor only if the combined delay t_{del} it takes to reach the detection voltage added to validation and protection system activation delay is short enough - typical time is 20 ms [49].

The system can be modelled as an electrical circuit of in series connected magnet's inductance (L), resistor corresponding to normal zone resistance and dump resistor (R_d). Thus, the coil current I can be computed from

$$L \frac{dI}{dt} + v_c(T, I) + R_d I = 0, \quad (6.1)$$

where v_c is the resistive voltage over the normal zone. Moreover, the choice of dump resistor value of 80 $\text{m}\Omega$ was based on the 1 kV voltage limit. This resistor value results in acceptable voltage over the dump resistor: 960 V at 12 kA.

This emphasises how the thermal and circuit problems are coupled: current in the circuit influences on the heat generation in the thermal problem whereas the temperature distribution in the magnet determines the voltage over the normal zone via temperature dependent resistive behaviour.

6.2 Simulation results

In this section we first present analysis for the nominal quench. From solutions of temperature and I as a function of time; resistive voltage, temperature distribution and normal zone evolution have been post-processed.

6.2.1 An analysis of the nominal quench

Parameters used in these computations are listed in Table 6.2. The protection system was activated after a protection delay (t_{del}) of 30 ms, after detection voltage (V_{det}) of 100 mV was observed.

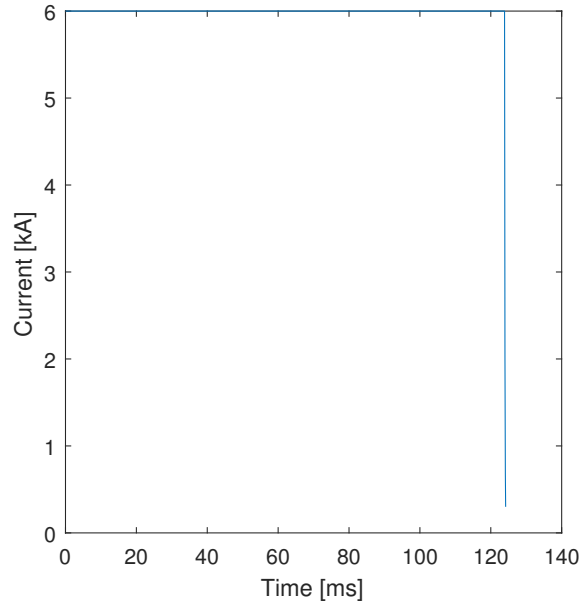


Figure 6.2. Coil current as a function of time. Current decreases to zero in 0.5 ms.

The current decay is shown in Figure 6.2. It takes only 0.5 ms for the current to decay down to 5% of I_{op} . The primary reason for this is the very low inductance of the magnet. The resulting resistive voltage is shown in Figure 6.3. The voltage over the whole magnet reaches its maximum value of ~ 0.5 V. Moreover the maximum temperature (hot spot temperature), shown in Figure 6.4, reaches 350 K.

In Fig. 6.5, the temperature distribution is presented when the hot spot temperature is at its maximum value, i.e., at the end of simulation. Temperature raise in the second and third cable, due to heat transfer through the insulation between the cable turns, can be observed also.

In Figure 6.6, the normal zone propagation is shown. Cable is determined to be locally in the normal zone, when the same amount of current flows in the stabilizer as in the superconducting layer itself. Other way to determine the normal zone according to the area that is above T_{CS} .

In Figure 6.7 the temperature distribution is shown in 3-D depiction of the coil. It is presented according to the modelling decision: cable's cross-section is isothermal. This visualizes well the temperature distribution in the magnet if compared to the 1-D temperature profile.

6.2.2 Critical current of the coil

In Figure 6.8, the coil's critical current is computed at different operation temperatures. This corresponds to average electric field of 10 mV/m. Magnet's critical current is impor-

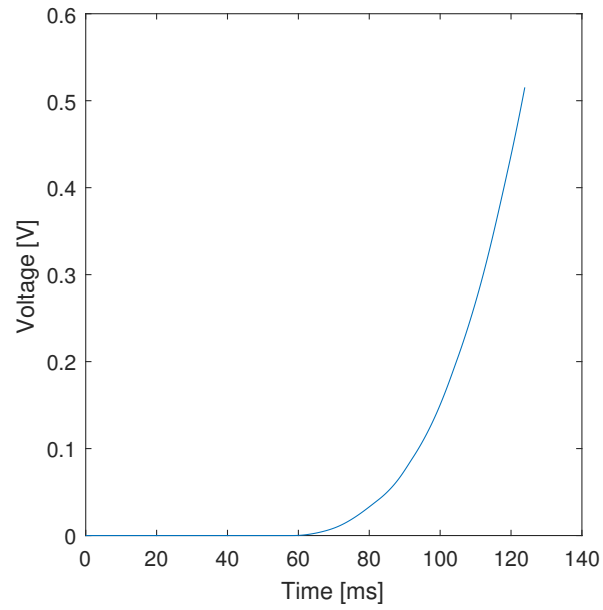


Figure 6.3. Coil's resistive voltage as a function of time.

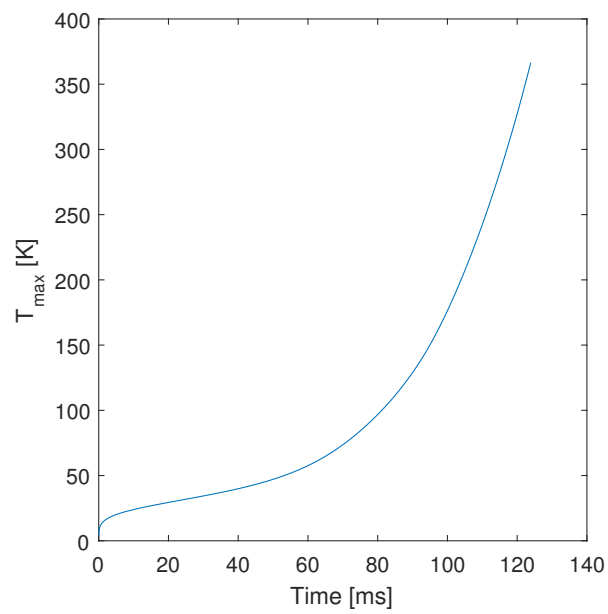


Figure 6.4. Hot spot temperature as a function of time.

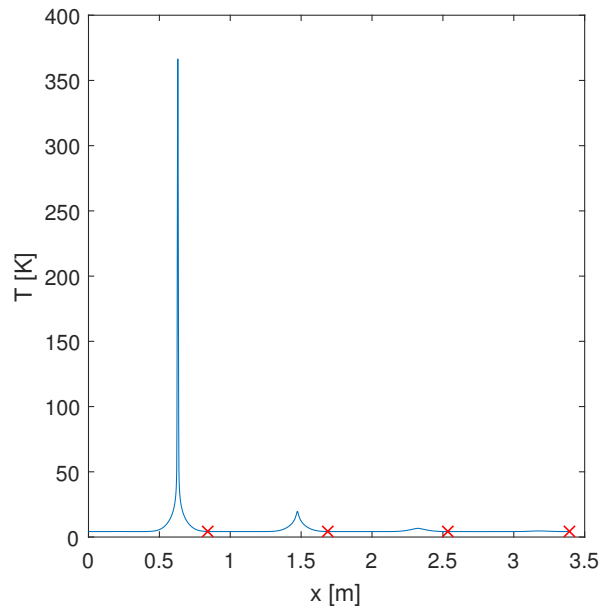


Figure 6.5. Temperature distribution along the coil length (x -axis), when hot spot temperature is at its maximum. The change of cable turn from previous to next one is marked with red crosses. The winding starts ($x=0$) from the middle of the straight part of the coil from the innermost cable turn.

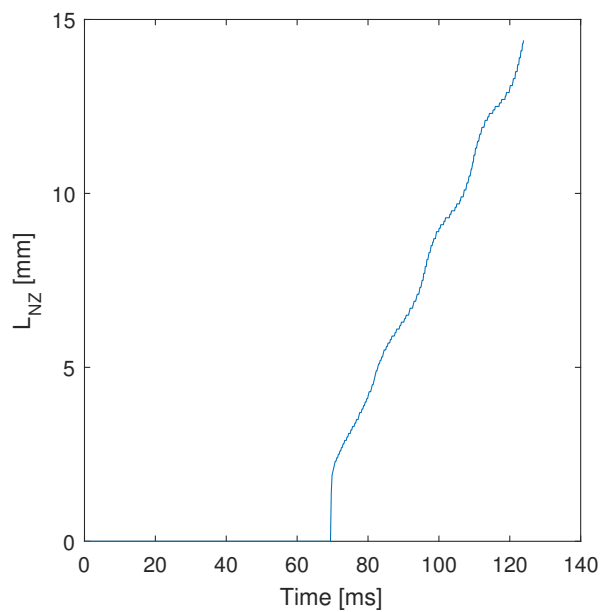


Figure 6.6. Length of the normal zone in the magnet as a function of time.

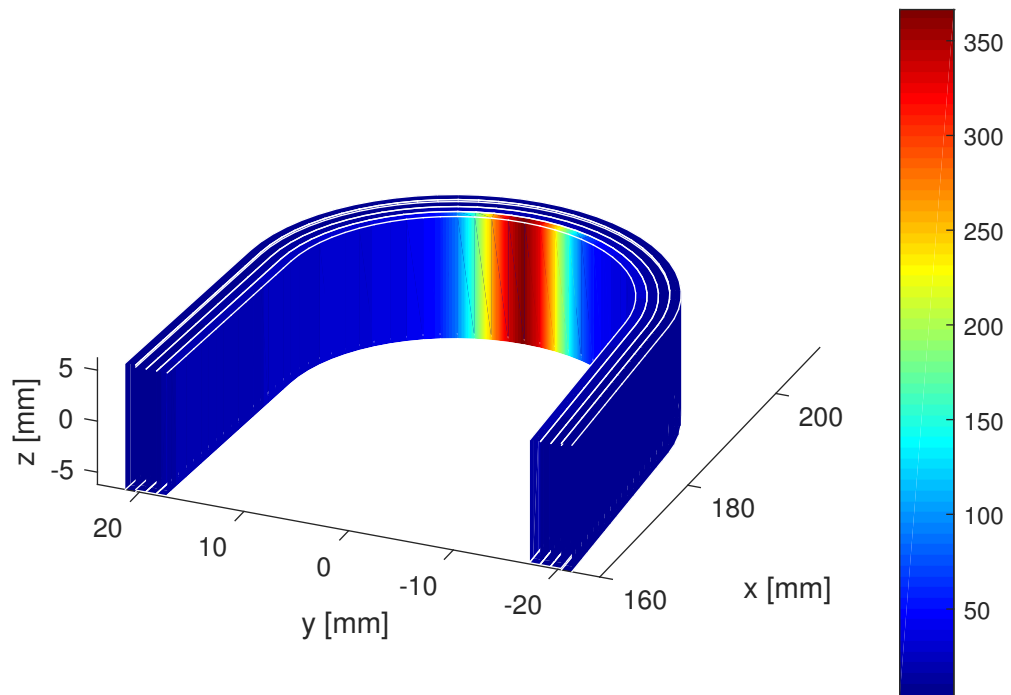


Figure 6.7. Temperature distribution in 3-D. Temperature colorbar on the right hand side in the figure is in Kelvins. The coil was quenched at the end of it in the first cable turn. $I_{op} = 6 \text{ kA}$, $t_{del} = 30 \text{ ms}$, $V_{det} = 100 \text{ mV}$.

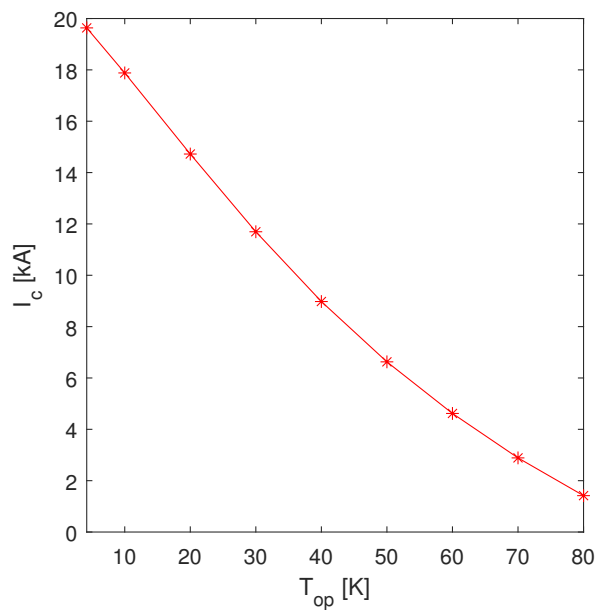


Figure 6.8. Predicted critical current of the coil at different operation temperatures. $V_{det} = 10 \text{ mV}$.

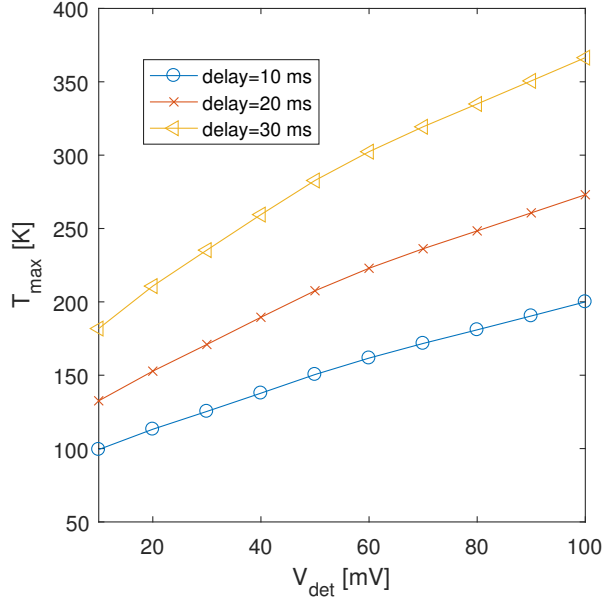


Figure 6.9. Maximum temperature as a function of detection voltage, with different quench protection system activation delays (t_{del}). $I_{op} = 6$ kA and $T_{op} = 4.2$ K.

tant to predict when designing superconducting magnets. It determines the current margin at which the device can be operated.

6.2.3 Varying detection voltage and switch delay

In this study, we investigate, how the quench detection voltage and quench protection system activation delay affect the hot spot temperature during the quench and protection. Typically, 300 K is considered to be the maximum allowed temperature in quench protection.

The maximum temperature as a function of V_{det} and t_{del} is then obtained and presented in Figure 6.9 and 6.10 for $I_{op} = 6$ kA and $I_{op} = 12$ kA, respectively - in both simulations T_{op} was 4.2 K.

To take a closer look at the maximum temperatures obtained at $I_{op} = 6$ kA ($\sim 0.3I_C$), with V_{det} varying between 10 and 100 mV and with t_{del} of 10, 20 and 30 ms (See Figure 6.9), the heat generation is moderate. Therefore more margin for detection is allowed. Even with delay of 30 ms and V_{det} of 100 mV the magnet can be protected.

In Figure 6.10 the same analysis is performed at I_{op} of 12 kA ($\sim 0.65I_C$). As intuitive, the heat generation is much more aggressive than at I_{op} of 6 kA. To limit the hot spot temperature below 300 K in case of V_{det} of 30 mV, the maximum protection delay is 10 ms.

In addition, at higher operation currents it is harder to protect the magnet due to switch delay of power electronics, therefore the speed of protection system has an immense impact

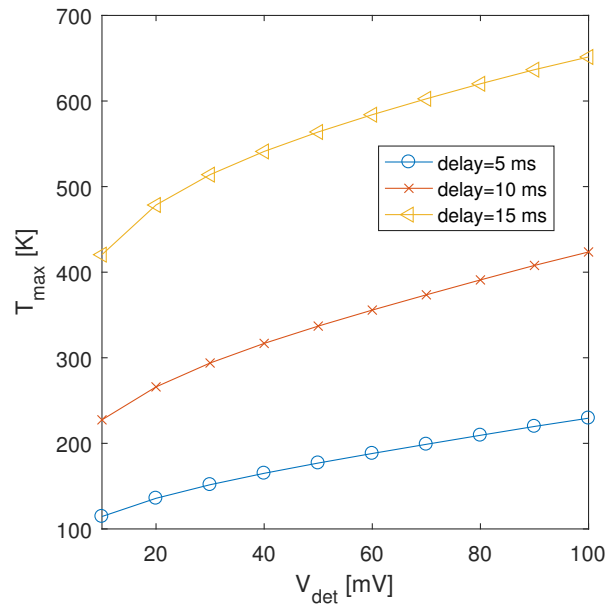


Figure 6.10. Maximum temperature as a function of detection voltage, with different quench protection system activation delays (t_{del}). $I_{op} = 12$ kA and $T_{op} = 4.2$ K.

on the fact whether a magnet can be protected or not.

7. CONCLUSIONS

Quench is an unwanted and irreversible thermal runaway, which is due to disturbance-caused transition of superconducting material from superconducting state into highly resistive one. If this occurs during operation of superconducting device, the system needs to be de-energized by activating the protection system in order to avoid breaking the device.

To ensure safe operation and to design magnet protection system in case of a quench, modelling is needed. Superconducting devices, like magnets, are large in size having structure consisting of anisotropic materials. Therefore, modelling quench in such devices can be time consuming if 3-D modelling domain is utilized. To simplify the problem, modelling decisions are taken when approaching the quench modelling computationally: One searches for appropriate approach for given situation where the representation of the modelling domain is simplified and essential physical phenomena are chosen. However, according to our current understanding, different quench problematics require different approaches and there is no tool that can tackle all the quench related problems - especially when we constraint the computation time.

In this work, a simulation tool based on a new approach, suitable for large superconducting devices, was developed to predict heat propagation during a quench. In the approach the heat diffusion equation was numerically solved for 3-D heat diffusion in 1-D modelling domain. To model temperature distribution along the cable only in 1-D, an assumption of isothermal temperature in cable's cross-section was deployed. FEM was utilized to model the heat diffusion along the cable and FDM was used to consider the transverse heat propagation.

To take the developed modelling tool in action a baseline of a prototype magnet series called Feather-M0, developed within EuCARD-2 project, was studied. In the simulations the requirements for quench detection and protection system were studied by parametric analysis for quench detection voltage and protection system activation delay. Based on the results, successful detection and short protection delay are of ample importance in HTS magnet protection. The time required to solve the quench problem was only couple minutes, while for 3-D FEM models solving the same problem would take several hours even. Furthermore, comparison with measurements is required to study the prospects of utilizing this tool in quench protection studies.

REFERENCES

- [1] American Superconductor Corporation
http://amsc.com/solutions-products/hts_wire.html
- [2] J. Bardeen, L. N. Cooper, and J. R. Schrieffer, "Theory of Superconductivity" *Physical Review* vol. 108, no. 5, 1957, pp. 1175-1204.
- [3] C. Barth, D. C. van. der. Laan, N. Bagrets, C. M. Bayer, K.-P. Weiss, and C. Lange, "Temperature- and field-dependent characterization of a conductor on round core cable" *Supercond. Sci. Technol.* vol. 28, no. 6, 2015, Art. ID. 065007.
- [4] E. Barzi, V. Lombardo, D. Turrioni, F. J. Baca, and T. G. Holesinger, "BSCCO-2212 Wire and Cable Studies" *IEEE Transactions on Applied Superconductivity* vol. 21, no. 3, 2011, pp. 2335-2339.
- [5] C. P. Bean, "Magnetization of hard superconductors", *Physical Review Letters*, Vol. 8, No. 6, 1962, pp. 250-253.
- [6] L. Bottura, "Stability of Superconductors" Superconductor Summer School Karlsruhe Germany, 2006.
- [7] L. Bottura, "A practical fit for the critical surface of NbTi" *IEEE Transactions on Applied Superconductivity* vol. 10, no. 1, 2000, pp. 1054-1057.
- [8] P. Bruzzone, "The index n of the voltage-current curve, in the characterization and specification of technical superconductors" *Physica C* vol. 401, no. 1-4, 2004, pp. 7-14.
- [9] G. Celentano *et al.*, "Design of an Industrially Feasible Twisted-Stack HTS Cable-in-Conduit Conductor for Fusion Application" *IEEE Transactions on Applied Superconductivity* vol. 24, no. 3, 2014, pp. 1-5.
- [10] The European Organization for Nuclear Research,
home page: <http://home.web.cern.ch/>
- [11] P. Eckels, "CryoComp Rapid Cryogenic Design: 88 Materials in Properties Database". Thermal Analysis Software.
- [12] J. Fleiter and A. Ballarino. "Parameterization of critical surface of REBCO conductors from Fujikura." CERN internal note, 2014, EDMS 1426239.
- [13] Fujikura Ltd. <http://fujikura.com/solutions/superconductingwire>

- [14] C. Geuzaine, and J.-F. Remacle, "Gmsh: A 3-D finite element mesh generator with built-in pre- and post-processing facilities" *International Journal for Numerical Methods in Engineering* vol. 79, no. 11, 2009, pp. 1309-1331.
- [15] A. Godeke, A. den Ouden, A. Nijhuis, and HHJ. ten Kate, "State of the art powder-in-tube niobium-tin superconductors" *Cryogenics* vol. 48, no. 7-8, 2008, pp. 308-316.
- [16] A. Godeke, B. ten. Haken, H. H. J. ten. Kate, and D. C. Larbalestier, "A general scaling relation for the critical current density in Nb₃Sn" *Supercond. Sci. Technol.* vol. 19, no. 10, 2006, pp. R100-R116.
- [17] W. Goldacker *et al*, "Status of high transport current ROEBEL assembled coated conductor cables" *Supercond. Sci. Technol.* vol. 22, no. 3, 2009, Art. ID. 034003.
- [18] W. Goldacker *et al*, "High current DyBCO-ROEBEL Assembled Coated Conductor (RACC)" *Journal of Physics: Conference Series* vol. 43, 2006, pp. 901-904.
- [19] W. Goldacker, F. Grilli, E. Pardo, A. Kario, S. Schlachter, and M. Vojenčiak, "Roebel cables from REBCO coated conductors: a one-century-old concept for the superconductivity of the future" *Supercond. Sci. Technol.* vol. 27, no. 9, 2014, Art. ID. 093001.
- [20] WV. Hassenzahl, DW. Hazelton, BK. Johnson, P. Komarek, M. Noe, and CT. Reis, "Electric power applications of superconductivity" *Proceedings of the IEEE* vol. 92, no. 10, 2004, pp. 1655-1674.
- [21] E. Häro, "Simulation Tool Development for Quench Modelling". Doctoral thesis, Tampere University of Technology, Tampere, Finland, 2016.
- [22] The magnetic fusion device project ITER,
home page: <https://www.iter.org/>
- [23] G. Kirby *et al*, "Accelerator-Quality HTS Dipole Magnet Demonstrator Designs for the EuCARD-2 5-T 40-mm Clear Aperture Magnet" *IEEE Trans. Appl. Supercond.* vol. 25, no. 3, 2015, Art. ID. 4000805.
- [24] Komarek, and E. Salpietro. "Review of European Activities in Superconductivity for Thermonuclear Fusion, in the Light of ITER." *IEEE/CSC & ESAS European Superconductivity News Forum.* Vol. 4. 2008.
- [25] D. Kottonau, E. Shabagin, M. Noe, and S. Grohmann, "Opportunities for High-Voltage AC Superconducting Cables as Part of New Long-Distance Transmission Lines" *IEEE Transactions on Applied Superconductivity* vol. 27, no. 4, 2017, pp. 1-5.

- [26] J. Kozak, M. Majka, and S. Kozak, "Experimental Results of a 15 kV, 140 A Superconducting Fault Current Limiter" *IEEE Transactions on Applied Superconductivity* vol. 27, no. 4, 2017, pp. 1-4.
- [27] V. Lahtinen, "Searching for Frontiers in Contemporary Eddy Current Model Based Hysteresis Loss Modelling of Superconductors". Doctoral thesis. Available online at: <http://urn.fi/URN:ISBN:978-952-15-3352-5>
- [28] V. Lahtinen and A. Stenvall, "Towards a unified framework for decomposability of processes." *Synthese*, 2016, 1-17.
- [29] M. Leghissa *et al*, "Bi-2223 multifilament tapes and multistrand conductors for HTS power transmission cables" *IEEE Transactions on Applied Superconductivity* vol. 7, no. 2, 1997, pp. 355-358.
- [30] J. Lehtonen, R. Mikkonen, and J. Paasi, "A numerical model for stability considerations in HTS magnets" *Supercond. Sci. Technol.* vol. 13, no. 3, 2000, pp. 251-258.
- [31] H. Maeda, Y. Tanaka, M. Fukutomi, and T. Asano, "A New High-TcOxide Superconductor without a Rare Earth Element" *Japanese Journal of Applied Physics* vol. 27, no. Part 2, No. 2, 1988, pp. L209-L210.
- [32] The National High Magnetic Field Laboratory.
<https://nationalmaglab.org/>
- [33] PJ. Masson, and CA. Luongo, "High Power Density Superconducting Motor for All-Electric Aircraft Propulsion" *IEEE Transactions on Applied Superconductivity* vol. 15, no. 2, 2005, pp. 2226-2229.
- [34] MATLAB, The MathWorks, Inc., Natick, Massachusetts, United States.
- [35] W. Meissner, and R. Ochsenfeld, "Ein neuer Effekt bei Eintritt der Supraleitfähigkeit" *Die Naturwissenschaften* vol. 21, no. 44, 1933, pp. 787-788.
- [36] K.-H. Mess, P. Schmüser and S. Wolff, "Superconducting accelerator magnets", World Scientific, 1996.
- [37] H. Miao, KR. Marken, M. Meinesz, B. Czabaj, and S. Hong, "Development of Round Multifilament Bi-2212/Ag Wires for High Field Magnet Applications" *IEEE Transactions on Applied Superconductivity* vol. 15, no. 2, 2005, pp. 2554-2557.
- [38] N. Mitchell *et al*, "The ITER Magnet System" *IEEE Transactions on Applied Superconductivity* vol. 18, no. 2, 2008, pp. 435-440.

- [39] A. Morandi, "State of the art of superconducting fault current limiters and their application to the electric power system" *Physica C* vol. 484, 2013, pp. 242-247.
- [40] J. Murtomäki, J. van Nugteren, G. Kirby, G. De Rijk, L. Rossi and A. Stenvall. "ICED An Inductively Coupled Energy Dissipater (ICED) for Future High Field Accelerator Magnets". To be published.
- [41] T. Nagaishi *et al*, "Development of REBCO coated conductors on textured metallic substrates" *Physica C* vol. 469, no. 15-20, 2009, pp. 1311-1315.
- [42] X. Obradors, and T. Puig, "Coated conductors for power applications: materials challenges" *Supercond. Sci. Technol.* vol. 27, no. 4, 2014, Art. ID. 044003.
- [43] R. J. LeVeque and J. Randall, "Finite difference methods for ordinary and partial differential equations: steady-state and time-dependent problems", Society for Industrial and Applied Mathematics, 2007.
- [44] E. Ravaioli, "CLIQ. A new quench protection technology for superconducting magnets", Universiteit Twente, 2015.
- [45] J. N. Reddy and D. K. Gartling, "The finite element method in heat transfer and fluid dynamics", Second edition, CRC Press LLC, 2001.
- [46] L. Rossi *et al*, "The EuCARD-2 Future Magnets European Collaboration for Accelerator-Quality HTS Magnets" *IEEE Trans. Appl. Supercond.* vol. 25, no. 3, 2015, Art. ID. 4001007.
- [47] L. Rossi *et al*, "The EuCARD-2 Future Magnets European Collaboration for Accelerator-Quality HTS Magnets" *IEEE Trans. Appl. Supercond.* vol. 25, no. 3, 2015, Art. ID. 4001007.
- [48] T. Salmi, "Optimization of Quench Protection Heater Performance in High-Field Accelerator Magnets through Computational and Experimental Analysis", Publication-Tampere University of Technology. Publication; 1311, 2015.
- [49] T. Salmi, and A. Stenvall, "Modeling Quench Protection Heater Delays in an HTS Coil" *IEEE Trans. Appl. Supercond.* vol. 25, no. 3, 2015, Art. ID. 0500205.
- [50] Multiple authors, edited by B Seeber 1998: "Handbook of applied superconductivity", IOP Publishing LTD, 1912.
- [51] Y. Shiohara, M. Yoshizumi, T. Izumi, and Y. Yamada, "Present status and future prospect of coated conductor development and its application in Japan" *Supercond. Sci. Technol.* vol. 21, no. 3, 2008, Art. ID. 034002.
- [52] A. Stenvall, T. Salmi, E. Härö, "Basics of Stability Analysis of Superconductors – What is it There Behind the Numerical Approaches and How They Can Be Utilized to Aid the Complete Superconducting Systems Engineering?", To appear.

- [53] A. Stenvall, "Platform for programming finite element method solvers in Matlab". <https://github.com/stenvala/dp>
- [54] A. Stenvall, A. Korpela, and R. Mikkonen, "Stability of MgB₂ Superconductor" *IEEE Trans. Appl. Supercond.* vol. 16, no. 2, 2006, pp. 1399-1402.
- [55] G. Strang and G. Fix, *An analysis of the finite element method*. Wellesley MA, Wellesley-Cambridge Press. 2nd ed., 2008.
- [56] SUite for Nonlinear and Differential/ALgebraic Equation Solvers (SUNDIALS), available online at: <https://computation.llnl.gov/projects/sundials>
- [57] SuperOx. <http://superox.ru/en/products/42-2G-HTS-tape>
- [58] SuperPower, Inc. <http://superpower-inc.com>
- [59] C. van Beijnen, and J. Elen, "Potential fabrication method of superconducting multifilament wires of the A-15 type" *IEEE Transactions on Magnetics* vol. 11, no. 2, 1975, pp. 243-246.
- [60] J. van Nugteren, *High Temperature Superconducting Accelerator Magnets*. Doctoral thesis, University of Twente, Twente, Netherlands, 2016.
- [61] J. van Nugteren *et al.*, "E³SPreSSO: A Quench Protection System for High Field Superconducting Magnets" CERN, TE-MS-C, Internal Note: 2016-23-v2, EDMS Nr: 1728301.
- [62] J. van Nugteren, "Internship Report: CERN, Software development for the Science and Design behind Superconducting Magnet Systems," tech. rep., University of Twente: Energy Materials and Systems and CERN: ATLAS magnet team, 2011.
- [63] K. Vinod, R. G. Abhilash. Kumar, and U. Syamaprasad, "Prospects for MgB₂ superconductors for magnet application" *Supercond. Sci. Technol.* vol. 20, no. 1, 2006, pp. R1-R13.
- [64] JO. Willis, "Superconducting transmission cables" *IEEE Power Engineering Review* vol. 20, no. 8, 2000, pp. 10-14.
- [65] M. Wilson, "NbTi superconductors with low ac loss: A review" *Cryogenics* vol. 48, no. 7-8, 2008, pp. 381-395.
- [66] M. Wilson, "Superconducting magnets", Oxford University Press, USA, 1987, 423 p.
- [67] M. Wilson, "NbTi superconductors with low ac loss: A review" *Cryogenics* vol. 48, no. 7-8, 2008, pp. 381-395.

- [68] Y. Xin *et al*, "Introduction of China's First Live Grid Installed HTS Power Cable System" *IEEE Transactions on Applied Superconductivity* vol. 15, no. 2, 2005, pp. 1814-1817.
- [69] G. B. Yntema, "Superconducting winding for electromagnet." *Physical Review* vol. 98, no. 4, 1955, pp. 1197-1197.
- [70] B. Zeitlin, G. Ozeryansky, and K. Hemachalam, "An overview of the IGC Internal Tin Nb₃Sn conductor" *IEEE Transactions on Magnetics* vol. 21, no. 2, 1985, pp. 293-296.
- [71] J. Zhao, A. Stenvall, T. Salmi, Y. Gao and C. Lorin, "Mechanical behavior of a 16 T FCC dipole magnet during a quench" *IEEE Trans. Appl. Supercond.*, 2017, In Press.
- [72] H. Zueger, "630kVA high temperature superconducting transformer" *Cryogenics* vol. 38, no. 11, 1998, pp. 1169-1172.